出國報告（出國類別：出席國際研討會發表論文）

# 出席「2010 美國航空太空學會航太科技研討會」會議報告

服務機關：國防大學理工學院
姓名職稱：洪健君 副教授
派赴國家：美國
報告日期：99 年 05 月 12 日
出國時間：99 年 04 月 17 日至 04 月 24 日

# 摘 要

本次會議為 2010 美國航空太空學會航太科技研討會，由美國航空太空學會(AIAA, American Institute of Aeronautics and Astronautics)主辦，美國航空太空總署 (NASA, National Aeronautics and Space Administration)協辦。本次會議發表的論文超過 220 篇，參加的各國學者家約 280 人。會議合計分三天進行，在 04 月 20 日至 22 日假美國喬治亞州亞特蘭大市(Atlanta, GA)之 The Westin Buckhead 飯店舉辦；會議主題為航太科技相關研究領域，本次研討會主要著眼於無人飛行載具(UAV, Unmanned Aerial Vehicle)及相關次系統，計有 12 子題分別進行相關領域探討。

本人此次為國科會航太學門研究計畫 NSC 98-2221-E-606-016 補助出席國際會議，所展示的研究內容及成果為提出以載人飛機之設計方法，進行小型無人飛行載具(Mini-UAV)之設計，以因應高酬載之設計需求，並由此逐步建立小型無人飛行載具的標準設計程序。會議期間除參與相關子題之會議研討外，亦與領域相關學者進行交流。

# 目　次

# 一、目的

本人此次出國爲國科會航太學門研究計畫 NSC 98-2221-E-606-016 補助出席國際會議，所發表的論文「以飛機設計方法進行小型無人飛行載具因應酬載需求之研究」(Study on Mini UAV Designs to Payload Requirements by Airplane Sizing Methodology)爲提出以載人飛機之設計方法，進行無人飛行載具 (UAV, Unmanned Aerial Vehicle)之設計，以因應高酬載之設計需求，並由此逐步建立小型無人飛行載具 (Mini-UAV)的標準設計程序。會議期間不僅參與相關子題之會議研討外，除進一步了解目前國際上對於無人飛行載具研究現況與未來發展方向，亦與無人飛行載具設計領域相關學者進行交流。希望藉由實際交流，進而建立合作契機，藉以增進研究績效。

# 二、過程

本次會議爲 2010 美國航空太空學會航太科技研討會 (AIAA Infotech@Aerospace - 2010 Conference and Exhibit)，本研討會係由美國航空太空學會(AIAA, American Institute of Aeronautics and Astronautics)主辦，美國航空太空總署 (NASA, National Aeronautics and Space Administration)協辦，美國航空太空學會及美國航空太空總署同爲全球航太科技相關研究領航的頂尖學術及研發機構，本次研討會亦爲國際間航太科技相關領域研究學者的年度盛事。本年度美國航空太空學會航太科技研討會在 04 月 20 日至 22 日假美國喬治亞州亞特蘭大市(Atlanta, GA)之 The Westin Buckhead 飯店舉辦。本次會議合計分三天進行，研討主題爲航太科技相關研究領域，本次研討會主要著眼於無人飛行載具及相關次系統，會議發表的論文超過 220 篇，參加的各國學者專家約 280 人，計有 12 子題分別進行相關領域探討。

本次赴美國參加研討會係發表研究論文「以飛機設計方法進行小型無人飛行載具因應酬載需求之研究」(Study on Mini UAV Designs to Payload Requirements by Airplane Sizing Methodology)，該篇論文之研究動機來自於帶領本校學生參加中華民國航空太空學會所舉辦的全國大專無人飛行載具設計競賽所獲得的理念。由於國內各大學之參賽機，無一架是按照典型飛機設計方法進行完成者，因此提供了本校參賽團隊一個良機；亦即，本校自 2006 年以來，嘗試以載人飛機之設計方法，設計小型無人飛行載具，以因應比賽時載重愈大愈好的需求，並由此逐步建立該型載具的標準設計程序，可應付未來其他需要。該論文先敘述典型載人飛機設計的程序，接著提出『此方法似可用於小型無人飛行載具之設計；只是需注意兩種飛行載具的不同點』，這些不同點是：(1) 呈現於兩者雷諾數的階數差一級，空氣動力學

的特性不同。(2) 設計初期，固然飛機主翼最大升力係數與翼剖面最大升力係數之間的關係，仍可適用於小型無人飛行載具，但建議採用雷諾數階數爲 5 之翼剖面氣動力係數，尤其以測試值爲佳。(3) 起飛距離性能需求，因小型無人飛行載具起降均在河岸進行，理應自美國聯邦航空法規 FAR 23 的限制中釋放出來，故遵循 FAR 23 之方法所得的馬力負載對翼面負載關係，必須加以修正。無人飛行載具以起飛總重分類，其等級範圍差異相當大，而對於起飛總重超過 2,000 磅等級無人飛行載具採用載人飛機相同概念與方法設計，可較爲人所接受。但是，對於起飛總重 10 至 99 磅等級無人飛行載具之設計，迄今仍無一明確設計概念與方法；本校以載人飛機設計概念發展小型無人飛行載具設計方法，歷經數次研發驗證已具相當可行性，然而運用於高酬載性能之小型無人載具設計，尚未實際驗證其可行性及適用性。因此，本次發表論文係運用此一設計概念及方法，執行高酬載性能之小型無人飛行載具設計及研製，進一步將可設計出一型具備高酬載及高操控性能之小型無人飛行載具，可供未來小型無人載具構型設計之參考。由於前述預計發表之論文係由大會安排在第三天 (04 月 22 日) 上午 11:30 之 71-1@A-71 議程才進行發表，所以在完成研討會報到程序後，本人即陸續針對與無人飛行載具設計研究相關領域之論文發表進行聆聽，希望對個人在此一領域研究之精進能有所助益。

本次研討會無人飛行載具設計研究相關領域共有 Unmanned Aircraft Design I & II 及 Unmanned Aircraft System Platforms I & II 等四個議程，其中由美國喬治亞理工學院 (Georgia Institute of Technology) 的 Jayant Ratti 等人所發表之 “Bio-Inspired Micro Air Vehicle: Design and Control Issues”係探討觀察昆蟲及鳥類的拍撲現象，進而發展出對於微飛行器(MAV, Micro Aerial Vehicle)的設計及飛行控制機制之精進，該篇論文之研究內容與本人目前與淡江大學共同進行之研究相關，也可以作爲日後研究之參考；在講員的精闢解說之後，也藉由與會學者熱烈討論中得知進一步研究概念，從演講內容之中實在獲益良多。

其次，另一篇由美國西密西根大學 (West Michigan University) 的 Kapseong Ro 教授等人所發表之 “Flight Testing of a Free- wing Tilt- body Aircraft” 則是在分享該大學所研製之無人飛行載具實機飛行測試與飛控模擬之驗證情形，該校所研製之 Free-wing Tilt-body 型無人飛行載具可以藉由改變機頭角度提供升力輔助，而無需大幅改變機翼攻角，亦不啻爲一有趣且值得注意之研究方向。再者，另一篇由美國堪薩斯大學 (The University of Kansas) 的 David A. Royer 等人所發表之論文 “Modeling and Sensitivity Analysis of the Meridian Unmanned Aircraft”，則是在探討該校研製之 Meridian 號無人飛行載具之飛控模式及靈敏度分析；美國

堪薩斯大學係飛行載具設計領域之巨擘 Dr. Jan Roskam 任教之學校，該篇論文與本校同樣使用 Jan Roskam 所發展之飛行載具設計軟體進行相關飛行參數之探討，可謂系出同門。只是該篇論文係導向討論飛行控制參數，與本人發表論文主要在探討飛行載具全機設計參數有所不同，不過仍有很大的參考價值。

大會最後一天 04 月 22 日上午安排本人論文在 71-1@A-71 議程進行發表，在發表論文之前亦前往相關領域論文發表場地聆聽各場次論文發表情形。其中來自日本東京大學 (University of Tokyo) 的 Takuma Hino 等人共同發表 "Formation Control of Small Unmanned Air Vehicles Under Faulty Communications" 及 "Research Activity on Unmanned Air Vehicles at the University of Tokyo" 兩篇論文，其內容主要在闡述該校歷年來所研發之各型無人飛行載具，並詳述其設計理念及參數驗證，在一張張投影片放映之下看到了該校對於無人飛行載具研發之用心及投入；看看別人想想自己，或許我國相關經費不及歐美等先進國家，然而那一份熱情及參與感，卻是我們可以好好學習的。由美國喬治亞理工學院 (Georgia Institute of Technology) 的 Wesley M. DeBusk 所發表之論文 "Unmanned Aerial Vehicle Systems for Disaster Relief: Tornado Alley" 則是分享該校對於無人飛行載具進行救災及空中監控之相關研究工作。由於無人飛行載具有低成本、功能性強及機動性高等特點，並可依不同任務需求酬載選用不同酬載，其主要應用範圍爲替代人員能執行危險(danger)、骯髒(dirty)、枯燥(dull)的任務；所以使用無人飛行載具進行反恐保安、搜索救難、交通監視、農漁業管理、空中攝影及電訊中繼等工作相當適宜，並且可以大幅降低救災人員傷亡，此點也可以由該篇論文得到驗證。本人在 11:30 至 12:00 發表論文之後，由於返國班機接駁及等待轉機時間的關係，只能再聆聽由 Yoo-Hsiu Yeh 所發表之 "Hardware Implementation of COTS Avionics System on Unmanned Aerial Vehicle Platforms" 論文，之後隨即在 12:30 攜帶由大會代爲保管之行李，搭乘地鐵趕赴亞特蘭大國際機場 (ATL, Atlanta Hartfield INTL) 轉機至達拉斯機場 (DFW, Dallas/Fort Worth INTL) 及洛杉磯機場(LAX, Los Angeles INTL)，再搭乘 04 月 23 日 00:10 起飛之長榮航空 BR15 班機於 04 月 24 日 05:30 抵台。

參與此次研討會受限於國軍人員差假規定，赴美國出差僅可在 3 天會議期程之外再加 5 天路程假；然而此次與會地點在美國東部，從台灣搭機出國往返美東非本國航空直航地區，單單在搭機及等待轉機時間即長達 60 小時以上！個人拙見以爲美國國土橫跨四個時區，如果美東及美西以相同之路程假標準恐有失公允，同時亦可能發生如同此次由於轉機等候因素而無法全程參與研討會之憾事。


圖 1　前往報到並在大會場地 The Westin Buckhead 飯店前留影

圖 2　研討會報到註冊情形 (一)

圖 3　研討會報到註冊情形 (二)


圖 4　論文發表前留影（一）


圖 5　論文發表前留影（二）


圖 6　投稿論文發表時段公告

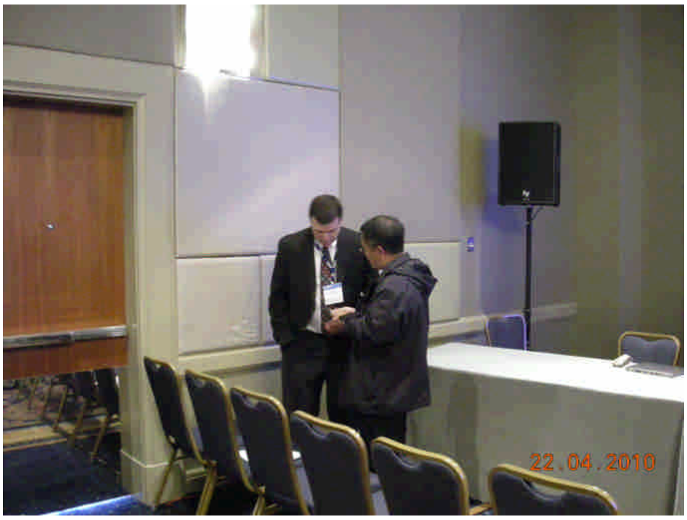


圖 7　論文發表前與會議主持人 Dr. Gregory H, Parker 交換名片並熱列討論情形


圖 8　論文發表準備情形

# 三、心得

此次與會從事相關研究人士均將其最新研究成果公開，並且各有其獨到見解；故參與此次會議可獲得目前最新的知識，使個人深覺獲益良多。經由本次的論文發表，使個人對未來研究更具信心。本研討會之目的主要爲探討航太科技等相關議題，尤其多所討論無人飛行載具及相關次系統之研發議題，所以參與本次會議可以各國專家學者討論問題之解析方法及經驗，不僅使個人在參與當中增廣見聞，對於問題的分析亦更加嚴謹。日後研究仍將一秉積極態度，期望能對相關領域研究的提升有所助益。在經歷國際學術會議洗禮後，個人專業能力得以成長；相信日後除了在無人飛行載具領域方面可以精進外，希望也可以整合個人另一微帶天線設計專長，進而達成無人飛行載具系統整合目標。

本次參與研討會亦親身體會到美國在科技方面的實力與進步，不論研究人才及研究經費都是令人稱羨。此次來到美國，發現去年在美國所看到經濟不景氣現象已有逐步改善跡象。洛杉磯國際機場國際航廈 Tom Bradley International Terminal 亦已整修完畢，給人耳目一新之感；整體洛杉磯國際機場航空貨運亦有起色，希望這一波美國經濟低迷現象能夠逐漸改善，也能夠進而帶動全球經際起飛。

# 四、建議事項

個人覺得國際交流是促進科技發展及學術成長的最佳途徑，國科會或相關機構應該提供足夠的經費推動國際學術活動，並且多鼓勵國內學者或研究人員踴躍參與國際會議。在參與此次會議後，發現先進各國對於參與此類學術活動相當熱烈，在在顯示參與各種國際會議或是相關學術交流活動，可以提升科技相關研究及產業發展。

# 五、攜回資料名稱及內容

1. AIAA Infotech@Aerospace - 2010 Conference and Exhibit 議事手冊 × 1
   ─ Final Program（發表論文時段如虛線標示處）

**Thursday Morning, 22 April 2010**

**69-I@A-69** — Software Systems II — Habersham

Chaired by: J. MURPHY, NASA Ames Research Center, Moffett Field, CA

| 1100 hrs | 1130 hrs | 1200 hrs | |
|---|---|---|---|
| AIAA-2010-3503<br>**Detecting Emergent Behaviors with Semi-Boolean Algebra**<br>P. Haglich, Lockheed Martin Corporation, Arlington, VA; L. Pullum, Ridge National Laboratory, Oak Ridge, TN; and C. Rouff, Lockheed Martin Corporation, Arlington, VA | AIAA-2010-3504<br>**A Comparison and Evaluation of Real-Time Software Systems Modeling Languages**<br>K. Evensen and K. Weiss, Jet Propulsion Laboratory, Padadena, CA | AIAA-2010-3505<br>**A New Software Engineering Course for Undergraduate and Graduate Students**<br>O. Jamathitikorn and L. Long, Pennsylvania State University, University Park, PA | |

**Thursday Morning, 22 April 2010**

**70-I@A-70** — Unmanned Aircraft System Platforms II — Ballroom C

Chaired by: G. PARKER, U.S. Air Force, Wright-Patterson AFB, OH

| 1100 hrs | 1130 hrs | 1200 hrs | |
|---|---|---|---|
| AIAA-2010-3506<br>**Unmanned Aerial Vehicle Systems for Disaster Relief: Tornado Alley**<br>W. DeBusk, Georgia Institute of Technology, Atlanta, GA | AIAA-2010-3507<br>**Study on Mini UAV Designs to Payload Requirements by Airplane Sizing Methodology**<br>C. Hung, C. Lin, Y. Teng, C. Chang and Y. Wu, National Defense University, Tahsi, Taoyuan, Taiwan (roc) | AIAA-2010-3508<br>**Hardware Implementation of COTS Avionics System on Unmanned Aerial Vehicle Platforms**<br>Y. Yeh, A. Ishihara and R. Lee, Carnegie Mellon Silicon Valley, Moffett Field, CA; P. Kumar, Polytechnic Institute of New York University, Brooklyn, NY; C. Ippolito, NASA Ames Research Center, Moffett Field, CA | |

**Thursday Afternoon, 22 April 2010**

1230-1400 hrs — Lunch

23

**Thursday Afternoon, 22 April 2010**

**71-I@A-71** — Applications Of Guidance, Navigation, & Control I — East Paces

Chaired by: D. ACCARDO, University of Naples "Federico II", Naples, Italy, and D. CLANCY, Lockheed Martin Corporation, Fort Worth, TX

| 1400 hrs | 1430 hrs | 1500 hrs | |
|---|---|---|---|
| AIAA-2010-3509<br>**The Design of Rapidly Reconfigurable Filters for Attitude and Position Determination**<br>R. Curry, M. Lizarraga, and G. Elkaim, University of California, Santa Cruz, Santa Cruz, CA | AIAA-2010-3510<br>**Autonomous Flight in GPS-Denied Environments Using Monocular Vision and Inertial Sensors**<br>A. Wu and E. Johnson, Georgia Institute of Technology, Atlanta, GA | AIAA-2010-3511<br>**Magnetorquer Based Attitude Control for a Nanosatellite Testplatform**<br>D. Toczynski, Stanford University, Palo Alto, CA; and R. Amini, Delft University of Technology, Delft, The Netherlands | |

**Thursday Afternoon, 22 April 2010**

**72-I@A-72** — Infotech R&D for Unmanned and Robotic Air Systems I — Ballroom C

Chaired by: M. FRANCIS, United Technologies Research Center, East Hartford, CT

| 1400 hrs | 1430 hrs | 1500 hrs | |
|---|---|---|---|
| AIAA-2010-3512<br>**Evaluating the Performance of a UAS-Based Precision Agriculture Imaging Payload**<br>D. Dvorak, J. Sorum, W. Semke, J. Neubert and R. Schultz, University of North Dakota, Grand Forks, ND | AIAA-2010-3513<br>**A Low Cost First-Person-View System for Remotely Operated Vehicles**<br>P. Marine and O. Rawashdeh, Oakland University, Rochester, MI | AIAA-2010-3514<br>**Dispatch Interface for Integration of Unmanned Aerial Systems into Public Safety Services**<br>W. DeBusk, C. Briton, M. Bigelow and K. Feigh, Georgia Institute of Technology, Atlanta, GA | |

2. AIAA Infotech@Aerospace - 2010 Conference and Exhibit 會議 online 論文集

PDF Papers Page 1 of 6

PDF Papers

Please select a title below to download as a PDF file

| Title | Year |
|---|---|
| 3-D Simulations for Testing and Validating Robotic-Driven Applications for Exploring Lunar Poles | 2010 |
| A Column Generation Approach to the Vehicle Routing Problem | 2010 |
| A Comparison and Evaluation of Real-Time Software Systems Modeling Languages | 2010 |
| A Conflict Resolution Algorithm For Reduced Controller Taskload | 2010 |
| A First-Person View System for Remotely Operated Vehicles Using a Fisheye-Lens | 2010 |
| A Graph-Based Approach to Situation Assessment | 2010 |
| A Hybrid Data-Model Fusion Approach to Calibrate a Flush Air Data Sensing System | 2010 |
| A Low Cost Phase Array Solution for UAV Collision Avoidance | 2010 |
| A Low-Cost Manipulator for Space Research and Undergraduate Engineering Education | 2010 |
| A Microwave Blade Tip Clearance Sensor for Propulsion Health Monitoring | 2010 |
| A Model Checking Example - Solving Sudoku using Simulink Design Verifier | 2010 |
| A New Software Engineering Course for Undergraduate and Graduate Students | 2010 |
| A Novel Anomaly Detection Technique based on Limited Anomalous Data | 2010 |
| A Review of Biologically Plausible Neuron Models for Spiking Neural Networks | 2010 |
| A Risk Assessment Architecture for Enhanced Engine Operation | 2010 |
| A Single Orbital Revolution Planner for NASA's EO-1 Spacecraft | 2010 |
| A Software Architecture for Autonomous UAV Mission Management and Control | 2010 |
| A Wireless Multiagent Architecture for Structural Health Monitoring that Incorporates Web Services | 2010 |
| Acoustic Emission Based Structural Health Monitoring of Stiffened Panels | 2010 |
| Adaptive Control Design for Longitudinal Aircraft Dynamics with Constrained Output Feedback | 2010 |
| Adaptive Control for Systems with Slow Reference Models | 2010 |
| Adaptive Control for the Generic Transport Model: A Derivative-Free Approach | 2010 |
| Adaptive Control Metrics via the Windowed Laplace Transform | 2010 |
| Adaptive Control of Quadrotor UAVs in the Presence of Actuator Uncertainties | 2010 |
| Adaptive Engine Control in the Presence of Output Limits | 2010 |
| Adaptive Feedforward Aircraft Control | 2010 |
| Adaptive Flight Control for Unmanned Aircraft Using a Stable Neural Network Observer | 2010 |
| Adaptive Load Control for Structurally Impaired Aircraft | 2010 |
| Advanced Sensor Systems for UAS Sense & Respond | 2010 |
| Aggregation of Uncertain Information in Distressed Aircraft Path Planning | 2010 |
| Airspace Statistical Proximity Maps Based on Data-Driven Flow Modeling | 2010 |
| An Algorithm for Enhanced Situation Awareness for Trajectory Performance Management | 2010 |
| An Event Detection Methodology for Identification of Aviation Mishap Leading Indicators | 2010 |
| An RTOS-Based Run-Time Reconfigurable Avionics System for UAVs | 2010 |
| Analysis and Asymmetric Sizing of CMOS Circuits for Increased Transient Error Tolerance | 2010 |
| Analyzing Distributed Functions in an Integrated Hazard Analysis | 2010 |
| Anomaly Detection Tool for ISHM | 2010 |

http://www.aiaa.org/PaperAccess/PDFPapers.cfm?CFID=19388414&CFTOKEN=849... 2010/4/20

附錄：「以飛機設計方法進行小型無人飛行載具因應酬載需求之研究」論文內容及研討會議程表（如後附）

— "Study on Mini UAV Designs to Payload Requirements by Airplane Sizing Methodology" & Final Program

# Study on Mini UAV Designs to Payload Requirements by Airplane Sizing Methodology

Chien-Chun Hung*, Chao-Hung Lin †, Yao-Jen Teng ‡, Chih-Ming Chang §, Yi-Kuang Wu**
*Chung Cheng Institute of Technology, National Defense University, Tahsi, Taoyuan, 33509, Taiwan ROC*

**The methodology for sizing airplanes that adapted to design uninhabited air vehicles with 20 to 50 pounds against payload goals is described in this paper. Focus is on importance of the unique characteristics of this sort of flying objects and how to deal with them. Features of several rivals designed to participate in Taiwan Robot Aircraft Design Competitions are discussed and further research is suggested finally.**

## I. Nomenclature

| | | |
|---|---|---|
| $A$ | = | aspect ratio, also, first constant of weight trend line equation |
| $P_{given}$ | = | given power |
| $\rho$ | = | air density |
| $R_N$ | = | Reynolds Number |
| S | = | wing area |
| $\sigma$ | = | ratio of air density at altitude to that at sea-level |
| $\overline{V}$ | = | tail volume coefficient |
| $W_E$ | = | empty weight |
| $W_F$ | = | fuel weight |
| $W_{TO}$ | = | take-off weight |
| $(W/P)_{TO}$ | = | power loading at take-off |
| $(W/S)_L$ | = | wing loading at landing |

## II. Introduction

THIS work was originally motivated by the need for helping senior undergraduate students to participate in an annual national UAV contest organized by Taiwan's Aeronautical and Astronautical Society of Republic of China. Competition rules set restrictions on the vehicle's size. All contestant UAVs weigh less than 50 pounds; therefore, they could be considered as the mini unmanned aerial vehicles (Mini UAV). The term "Mini UAV" used here means all the uninhabited aerial vehicles with take-off weight of 5 to 50 pounds (2.27 kg to 22.67 kg) as categorized in Weibel's paper.[1] Over the past years since it began, no team designed its aircraft exactly by the process discussed in any typical textbook. People prefer to make the rival aircraft by using concepts as for fabricating model airplanes. Doing that way is easier than utilizing airplane design methodology to finish the job since players' experience could dominate and using the latter could cause some academic troubles. However, from the point of view of being a teacher, students should be not only guided to win the award but also taught to practice via the contest what they learned in the course "Airplane Design" to draft their UAVs for the competition. Being eager to win is one thing, reaching the educational goal is the other, and, the most important. The students should be

* Corresponding Author, Associate Professor, Department of Mechatronic, Energy and Aerospace Engineering, AIAA Member, Email: hung@ndu.edu.tw.
† Adjunct Associate Professor, Department of Mechatronic, Energy and Aerospace Engineering, AIAA Member.
‡ Consultant, Who Flies Mini-UAVs And Instructs Students to Make Them; Also A Graduate Student in Doctoral Program of School of Defense Science, Non-member.
§ Graduate Student in Master Program, Department of Mechatronic, Energy and Aerospace Engineering, Non-member.
** Graduate Student in Master Program, Department of Mechatronic, Energy and Aerospace Engineering, AIAA Student Member.

educated to become skilled at the formal methodology even when they are dealing with model airplanes, or we might call those things mini UAVs. We must get through those troubles to develop a new way for our students to design their competition UAVs and this is why this paper comes out.

## III. Taiwan Unmanned Aerial Vehicle Design Competition

The Aeronautical and Astronautical Society of Republic of China in TAIWAN hosts an Airplane Design Competition for its student members every year since 1999, then to expect all the draft aircraft aloft, this contest focused on remotely piloted vehicles and later changed its name as "The Domestic College Student's Unmanned Aerial Vehicle Design Competition." In 2008, another name "2008 Taiwan Unmanned Aerial Vehicle Design Competition" was announced to attract high school students, even foreign teams, to join. Now,* it is called "2010 Taiwan Robot Aircraft Design Competition."

There are several Championships to award in this Competition: Beginners', Advanced Level's, Flapping-Wings', and Beyond Visual Ranges' (BVR). Although the organizer now welcomes all participants to enroll all contests, the first three authors considered the previous arrangement as it should be, that is, Beginners Division for juniors, Flapping-Wings and BVR supposed for graduate students. Therefore, due to their ability and the opportunity to practice what they learn in the course "Airplane Design," our senior undergraduate students are encouraged to participate in the Advanced Level Design Contest. Stories are all about this level.

## IV. Contest Rules and Mission Specifications

In the Advanced Level Design Contest, each competing aircraft must be aloft using an assigned piston engine with maximum power of 2.8 hp at 15000 rpm for a required minimum period. It is then scored by its flight evaluations (according to the maximum payload it carried, the fuel it consumed, and its configuration), the design report (paper and oral work), and the fabrication and demonstration skill. In addition, the team that demonstrates its UAV with the most outstanding aerodynamic shape can be awarded the Aerodynamics Trophy with no need to do any flight exhibition. The contest rules were modified occasionally and are properly settled recently. Table 1 shows how the design competition rules for this title were modified year by year since 2007.

To give students an appropriate concept that they simply cannot design a cargo airplane with the F-16 configuration, we strongly recommend them focus merely on payload requirements. While development of the adoption of airplane sizing method for mini UAV is still carrying on, we welcome the conventional configurations as their designs. Since working on the mission profile is a good place to start the design, as shown in many textbooks, all of our competing students have to use the contest rules for setting-up their mission specifications followed by mission profiles. The designer† of Year 2007 answered it by using a mission profile exactly the same as given in Figure 2.1 of Ref. 2 (exclusive of the Loiter Phase) with the following specification:

1) Payload: 6 kg (13.2 lb).
2) Range: 2 km (1.079 nm). While mission finished, 25% of required fuel reserved.
3) Altitude: Cruise at 100 m (328 ft). Maximum at 300 m (984 ft).
4) Cruise Speed: 70 km/h (19.4 m/s, 63.8 fps) with full payload.

Most followers did their designs by keeping this specification but with slight modifications, say, the payloads increase every year and a longer range of 2500 m (8202 ft) has been used from Year 2008 to present.

Table 1 Taiwan UAV Design Competition, Outline of Advanced Level Title Rules.

| Year | Wing Span, b | Total Lifting Area (Wing and Horizontal Tail) | Take-off Ground Run, [1] $S_{TOG}$ | Landing Distance, $S_L$ | Minimum Payload Required |
|---|---|---|---|---|---|
| 2007 | Non-regulated | ≤ 2 m$^2$ (21.53 ft$^2$) | ≤ 60 m (196.8 ft) | Regulated to land within an assigned zone | 4 kg (8.81 lb) |
| 2008 | Non-regulated | ≤ 2 m$^2$ (21.53 ft$^2$) | ≤ 60 m (196.8 ft) | < 200 m (656.1 ft) | 4 kg (8.81 lb) |
| 2009 | ≤ 350 cm (11.48 ft) | Non-regulated | ≤ 60 m (196.8 ft) | < 200 m (656.1 ft) | 4 kg (8.81 lb) |
| 2010 | ≤ 300 cm (9.84 ft) | Non-regulated | ≤ 60 m (196.8 ft) [2] | < 200 m (656.1 ft) | 5 kg (11.02 lb) [3] |

[1] This is for the maximum-payload race only. The ground run limit is set to be 100 m (328.1 ft) for the lowest-fuel-consumption race.
[2] In the maximum-payload race, those vehicles that take-off out of 60 m bound will be dismissed and scored nothing.
[3] Compared with the self-recorded amount of payload attempted at home, the contest allows each competitor put only 2 kilograms (4.4 lb) extra in the air.

*URL: http://www.iaa.ncku.edu.tw/~whlai/uav/index.html [cited 4 March 2010].
†Po-Yu Cheng, Designer of "One-Piece," Student of Class 2007.

# V. Adoption from Airplane Sizing Methodology to Mini UAV Design

Any one who has examined the basics of airplane sizing methodology[2-6] may possibly find that the equations used will go into three categories. They are about weights, about correlating data, and about the aerodynamics. For aerodynamics, even we have to deal with some coefficients that are dependent on Reynolds number; it is obvious that force equilibriums are considered first, and then these coefficients will appear by dimensionless treatments, no matter what the flight object's size is. If we can develop an unique fuel-fraction method[2] and construct the correlating database especially for the mini UAVs, then we will see the possibility of using airplane design method to size mini unmanned aerial vehicles.

Most mini UAVs fly at Reynolds number in a range of $10^5$ to $10^6$ (based on mean geometric chord length of wing, MGC) while airplanes above $10^6$. With Reynolds numbers from $10^5$ to $10^6$, the lift-to-drag ratio increases more than one order of magnitude for smooth airfoils. It does not change this abrupt but still has couples of multiple increasing for rough airfoils.[7] The section maximum lift coefficient increases more than 30% for some symmetric airfoils with this variation of $R_N$ (Fig. 9.3, Ref. 5). Using airplanes' data for aerodynamic calculations in mini UAVs is somewhat overestimated. However, if the aerodynamic coefficients appropriate for them in this regime ($10^5 \le R_N \le 10^6$) are determined, it will be reasonable to design mini UAVs by applying the airplane sizing methodology, especially in performance matching and stability evaluations.

## A. Design Process

In his paper, Anderson[8] cites Raymer's description[3] about the methodology for conceptual airplane design as the following successive process: Once the requirement is established, a first estimation of take-off weight frequently based on the previous aircraft can be made. The necessary critical performance parameters (such as maximum lift coefficient, lift-to-drag ratio, wing loading, and power loading) are determined. An initial configuration layout is then prepared. At this moment, a group of weights (including take-off weight, empty weight, and so on) is approximately calculated and this will result in a better weight estimate. Then a performance analysis can be carried out to check the requirement is met or not. If not, re-determine the critical performance parameters and proceed to the above successive steps until it meets the requirement. Finally as the proceeding iterative process reaches its end, the designers might think about an optimization procedure to obtain the best design.

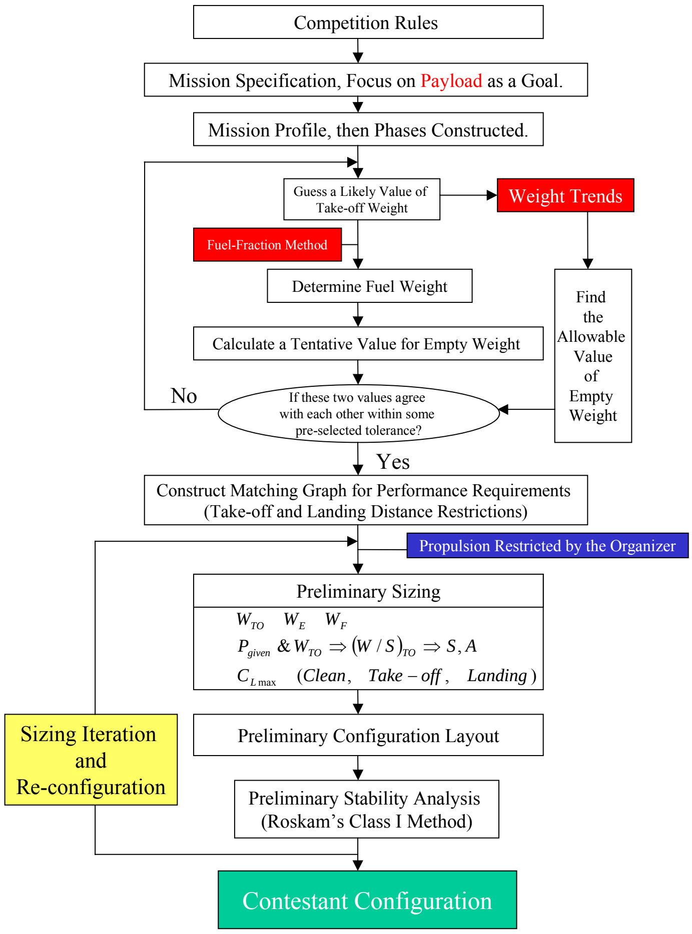


**Figure 1. Mini Unmanned Aerial Vehicle (Mini UAV) Design Process.** *Details are discussed in the text.*

For mini UAVs, or especially for Taiwan Robot Aircraft Design

Competition, shown in the flow chart of Fig. 1 (modified from Figure 1.2 of Ref. 2), we propose a design process adapted from that of airplanes. It is similar to that of sizing an airplane in which the take-off weight is first estimated by comparing two empty weights from a guessed value of it, one obtained by the fuel-fraction method[2] while the other by the trend line representing regression bases on historical mini UAVs' weight data. Iteration is needed if the difference between two quantities is not within a given tolerance.

After the weight estimation, a performance-matching plot is constructed to fit the take-off distance, the landing distance constraints with an assigned horsepower. Before further researches on them, Federal Aviation Regulations Part 23 (FAR 23) is applied so far to size mini UAVs. From the matching graph, the take-off power loading, take-off wing loading, maximum lift coefficients, and aspect ratio, can be selected. With these known data on hand, we can do the preliminary configuration layout. As usual, a designer must have some historical data of the same type of aerial vehicles to fulfill it. Grouping and adding many existing mini UAVs to those 12 types to form a new type, Type 13, in Ref. 2 for this usage might be necessary. Rather than putting others together, it would be better grouping our own vehicles for this purpose as discussed later.

With the preliminary configuration, by Class I Stability Analysis as described in Ref. 4, longitudinal X-plot and directional x-plot are used to see if the empennage match the inherent stability goal or not. If it does not, then go back to the Preliminary Configuration Layout process and do the re-configuration.

In this work at the beginning, there was almost nothing available for sizing-reference; therefore, the designer of Year 2007's had no choice using some analogous data from Type 2 airplanes of Ref. 2 and the contestant UAV in Year 2006. (That one was made by students under instruction of the third author according to his model-airplane

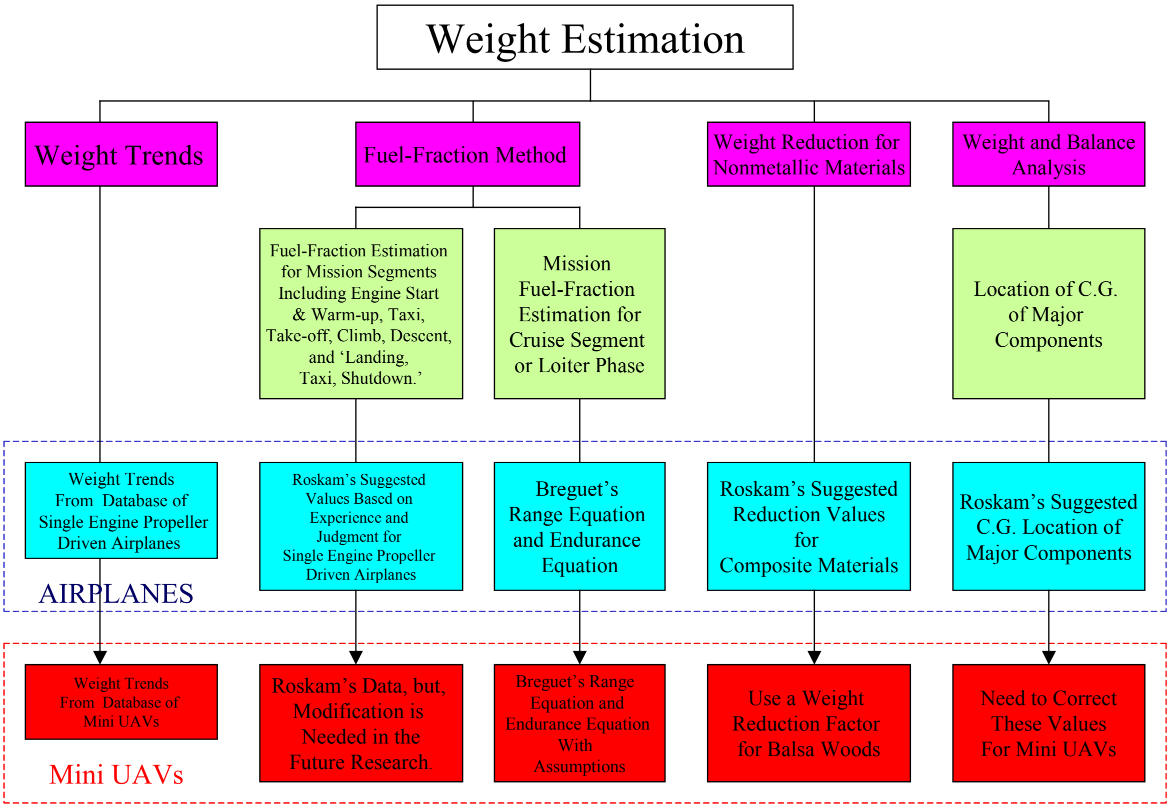


**Figure 2. Keys for adoption of airplane sizing method to mini UAVs.** *These blocks show the idea how airplane take-off weight approximation is modified for mini UAV sizing.*

experience.) Successors were lucky simply because they have at least two UAVs that can be referred to. In addition, due to the tight schedule, few undergraduate designers can enter the iteration and re-configuration process.

It is clear that what have been shown in this design process is nothing but more like that for sizing an airplane. The difference between these two kinds of aerial vehicles will be emphasized while the details of adaptation reveal.

## B. Weight Estimation

There are five items need to be adjusted for mini UAVs in this category (Fig. 2):

1) Weight Trends.
2) Fuel-Fraction Guessed for phases excluding Cruise (and/or Loiter) Segment.
3) Breguet's Range and Endurance equations.
4) Weight Reduction for wood used in this type of air vehicles.
5) Center of Gravity (C.G.) Location for major components in this type of air vehicles.

Ref. 2 ensures that there is a linear relationship between $\log_{10}W_E$ and $\log_{10}W_{TO}$ for twelve types of airplanes. The truth is also assumed for mini UAVs. To obtain $W_E$ from $W_{TO}$, regression analysis must be done to offer this relationship by collecting available data from current mini UAVs.

It is not difficult to calculate mission fuel weight by Fuel-Fraction Method[2] if the fuel-fractions of all phases are found. As shown in Ref. 2, Breguet's range and endurance equations combined with a set of suggested values for phases excluding Cruise and Loiter are used to perform this approximation for all twelve types of airplanes, but not for mini UAVs. In this case, being short of real statistical data for phases excluding cruise and loiter makes the estimation less precise. Before the measured values are obtained, the better way is to borrow those recommended values for Type 1 or Type 2 airplanes as shown in Table 2.1 of Ref. 2.

Since with just the concept of fuel-consumption rate, time and speed, one can derive both the Breguet's range and endurance equations, possibility of applying them on mini UAVs exists except that the fuel-consumption rate for their engines should be experimentally determined in the beginning.

Wood is the major construction material of our mini UAVs while all almost airplanes in Ref. 2 were made of metals and/or composite materials. Weight reduction should follow due to material difference even with the same estimating method. A reduction factor was found to be 0.442 especially for this group's vehicles and how came this value will be discussed later.

Table 10.2 of Ref. 4 gives us good information about the C.G. location of major components before the air vehicles is made in real, it is beneficial to know these values since the empennage sizing will use them to construct the longitudinal and directional x-plots. Comparing the manufacturing techniques of both airplanes and our competing mini UAVs, the significant difference will be that our students are not actually professional in making aerial vehicles while those who fabricate airplanes are. Therefore, these C.G. location data from airplanes did introduce some discrepancy while applied to mini UAVs. Correction should be necessary.

## C. Matching Plot Regarding Special Constraints

Probably because of being for educational purpose, the first two authors make it simple by not introducing too many design restraints on students' mini UAVs. The coincidence is that the organizer announces not many constraints for the competing flight objects. After evaluation of rules, two margins were placed on the matching graph in the performance analysis. With these two restrictions, the take-off and landing distances as barriers, Ref. 2 teaches the student designers how to chart the power loading versus wing loading diagrams, from which young engineers can select an initial design point to keep their individual work in progress.

If we consider a mini UAVs as the tiny replica of single engine propeller-driven airplane, then FAR 23 can be used to constrain the distances. The take-off ground run, $S_{TOG}$, is proportional to the so-called take-off parameter for FAR 23 airplanes, $TOP_{23}$, defined by Eq. (1),

$$TOP_{23} = (W/S)_{TO}\,(W/P)_{TO} \,/\, \sigma\, C_{L_{max_{TO}}} \tag{1}$$

where $(W/S)_{TO}$ is the wing loading and $(W/P)_{TO}$ the power loading at take-off. The take-off and landing distance of our vehicles should be more loosely-constrained since they need not climb out above the obstacle of 50 ft as regulated by FAR 23. The whole mission is carried out within the riverside regions where are much less inhabited and it will not be a threat to any urban personnel or building. A new relationship between the take-off ground run $S_{TOG}$, and take-off parameter $TOP_{23}$, is probably needed in future studies (Fig. 3).

On the other hand, the landing distances for FAR 23 airplanes are related to the landing stall speeds, which depend on the maximum landing lift coefficients. The power-off landing stall speed, $V_{S_L}$, is as shown in Eq. (2).

$$V_{S_L} = \{2\,(W/S)_L \,/\, \rho\, C_{L_{max_L}}\}^{1/2} \tag{2}$$

Then in the matching graph, the chosen design point determines the maximum take-off lift coefficient and the maximum landing lift coefficient, with a now prescribed pair of take-off power loading and wing loading values.

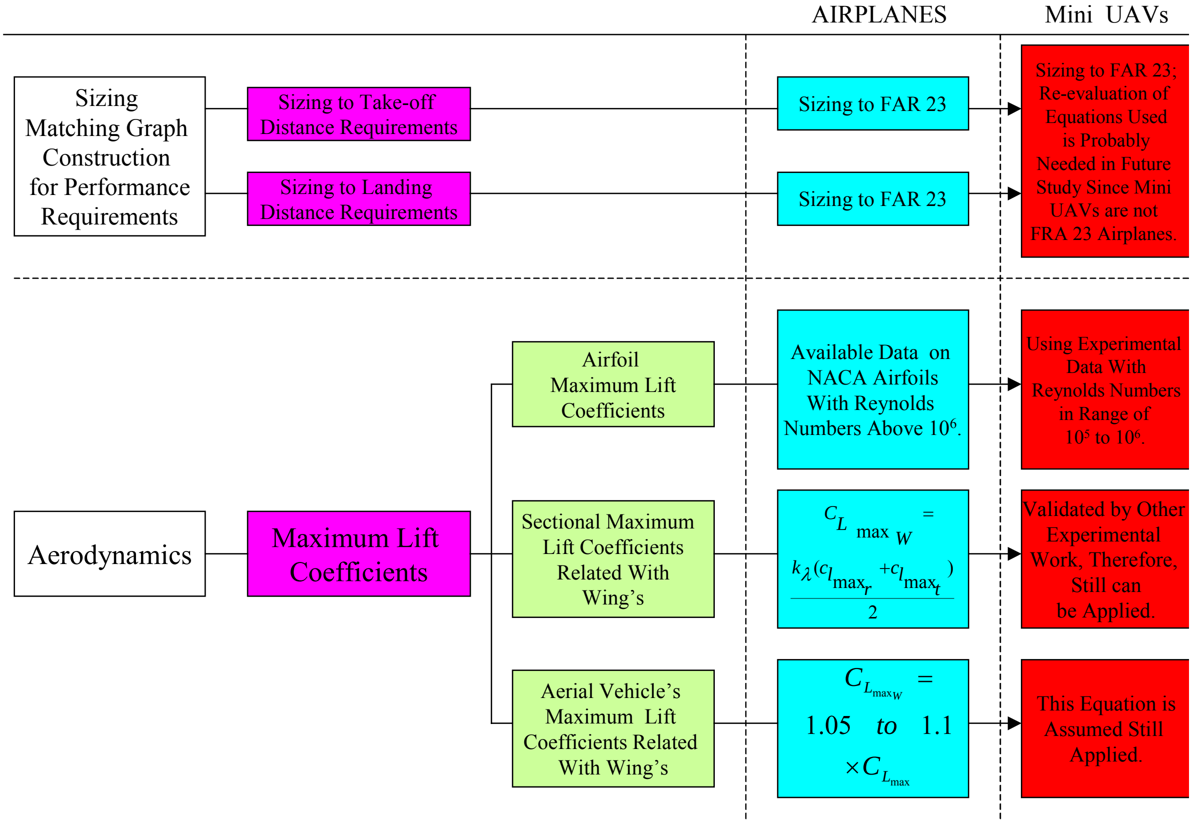


**Figure 3. Keys for adoption of airplane sizing method to mini UAVs (Cont'd).** *These blocks show the idea how to adapt both the matching for performance requirements and selection of airfoils to fit the calculated maximum lift coefficients.*

### D. Low Reynolds Number Aerodynamics

Selection of airfoils to provide sufficient lift for an airplane is a very important step to size them. The maximum lift coefficient for airplane, $C_{Lmax}$, decided to satisfy the performance requirements should be magnified to the maximum lift coefficient for wing, $C_{Lmax_W}$, by Eq. (3).[4] It is because of the trim considerations for conventional configuration as well as for with canard, the factors 1.05 to 1.1 will be chosen depending on how far the horizontal stabilizer is from the center of gravity. We can simply assume that this is the case for our mini UAVs since so far it seems to us difficult to check it experimentally.

$$C_{Lmax_W} = 1.05 \text{ to } 1.1\ C_{Lmax} \tag{3}$$

The section maximum lift coefficient, $c_{l_{\max}}$, should be obtained using Eq. (4) from the maximum lift coefficient for wing,[4]

$$C_{Lmax_W} = k_\lambda \left(c_{l_{max_r}} + c_{l_{max_t}}\right) / 2 \tag{4}$$

where $k_\lambda$ is taper ratio correction factor for wing maximum lift coefficient obtained from historical airplane data, and $k_\lambda$ is 0.88 for $\lambda = 1.0$ as 0.95 for $\lambda = 0.4$. Here, $\lambda$ is the taper ratio. In Eq. (4), $c_{l_{max_r}}$ and $c_{l_{max_t}}$ are the section maximum lift coefficients of wing root and tip airfoils, respectively. As mentioned in Section V, these two different kinds of air vehicles fly at distinctive Reynolds numbers, applicability of Eq. (4) to mini UAVs should be checked. Fortunately, it is shown still valid for his mini UAV with two typical low speed airfoils at Reynolds number about

$10^5$ by the fourth author* using another previous experimental work.† Up to now, it is appropriate for us to apply any available airfoils that hold their wind tunnel testing data with Reynolds numbers in the range of 1 x $10^5$ to 1 x $10^6$. This concept of low Reynolds number aerodynamics is the key point to illustrate the uniqueness of a mini UAV as showing in Fig. 3.

### E. Mini UAV Configuration Sizing

As shown in Fig. 4, for shaping the preliminary aerodynamic profiles is just utilizing the previous wing and fuselage data of mini UAVs with the thus-far known values. It is obvious that this is the same as to design inhabited air vehicles. For both wing and fuselage configuration drawings, earlier mini UAVs, especially of our group, are good examples to follow and with continuing modifications on them if necessary. For empennage sizing of our mini UAVs, the so-called tail-volume coefficient method[4] first based on Types 1 and 2 airplanes of Refs. 2 and 4, later on our gradually developed mini UAVs' database is used.

### F. Stability Analysis

Chapter 11 of Ref. 4 suggests a fast way to analyze whether an airplane configuration has the satisfactory stability or not. In short, the longitudinal X-plot and the directional X-plot are constructed to see if the planned empennage sizing could fit to the needs as shown in Eqs. (5) and (6). A longitudinal X-plot presents the variation of aerodynamic center and center of gravity as a function of horizontal tail (canard) area. Using thus-far known aerodynamic profile data and the suggested values of c.g. location data for major components and whole vehicle, these X-plots can be constructed. For the longitudinal X-plot, aerodynamics analysis and weight and balance analysis are necessary. For the latter, Table 10.2 of Ref. 4 provides good correlating data for c.g. location of major components. On the other hand, the directional X-plot places the variation of derivative of airplane yawing moment coefficient with angle of sideslip as a function of the vertical tail area.

It is recommended that in the preliminary design phase for an airplane to be inherently stable, Eq. (5) holds for longitudinal stability while Eq. (6) is for directional stability.[4]

$$S.M. = dC_m / dC_L = \bar{X}_{cg} - \bar{X}_{ac} = -0.10 \quad (5)$$

$$C_{n_\beta} = 0.0010 \text{ per degree} \quad (6)$$

In Eq. (5), S.M. means static margin, $C_m$ the pitching moment coefficient, $C_L$ the lift coefficient, $\bar{X}_{cg}$ the distance from leading edge of wing mean geometry chord to center of gravity in fraction of $\bar{c}$, the chord length of MGC. In addition, $\bar{X}_{ac}$ is the distance from leading edge of wing mean geometry chord to aerodynamic center in fraction of $\bar{c}$ and $C_{n_\beta}$ is the yawing-moment-coefficient-due-to-sideslip derivative.

As mentioned before, equations of motion (dealing the equilibriums of flight vehicles) are always the beginning work of the aerodynamics and stability analysis. In our design

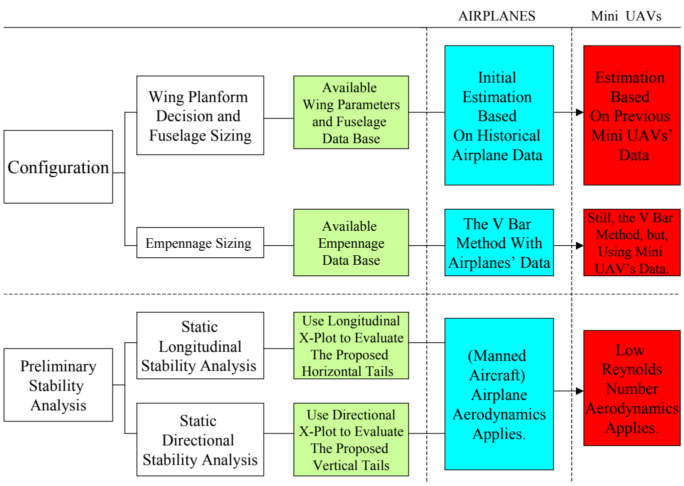


**Figure 4. Keys for adoption of airplane sizing method to mini UAVs (Cont'd).** *These blocks show the ideas how configuration and preliminary stability analysis process are modified for mini UAV sizing.*

---

*In His Master Degree Thesis That Will Appear in This May, Written in Traditional Chinese, March 2010.

†Chang-Chieh Wu, "Investigation of Aerodynamics Characteristics of Low-Reynolds Number Wings for Micro Aerial Vehicles," Rept. NSC 90-2623-7014-013, National Science Council, Taiwan, R.O.C., March 2002. (In Traditional Chinese)

work for mini UAVs, the above-issued X-plots can no doubt be applied to do the jobs since the low Reynolds number aerodynamics has been used to character this type of air vehicles.

## VI. History of Development of Our Vehicles

The following is the summary of how this work approaches the above-mentioned during those days from the year 2006 to present.

First design came out in 2007, named One-Piece, with an assumption that mini UAVs can be sized by the same methods used in drafting Type 2 of Roskam's airplane category.[2] We originally specified a requirement with 13.2 pounds payload at that time. Also according to the rules set by the contest organizer, a mission profile was defined by breaking it down into seven phases, including engine-start and warm-up, taxi, take-off, climb, cruise, descent, landing and shut-down. The take-off weight was estimated by the fuel-fraction method[2] while the fuel fraction of each phase except Cruise Phase was assumed to be the same value used in Type 2 airplanes, the single piston engine driven airplanes. Mini UAVs used in the regression line for empty weight versus take-off weight were picked from Jane's online *All the World's Aircraft.*[9] The actual take-off weight of One-Piece was reduced by a factor of 0.442 from the calculated value to compensate for the material difference between it and those preceding mini UAVs. One-Piece won the first prize aloft with a dead weight of 15.10 pounds (designed for 13.23 pounds payload) and it showed the possibility of this idea (as the title is talking about).

Once the likelihood became clear, those mini UAVs used for establishing the regression line of $\log_{10}W_E$ versus $\log_{10}W_{TO}$ were moved, instead, the weight quantities of domestic participant UAVs were placed on the weight trend line. The payload was up by amount of 2 pounds and the wing was changed to be low. Many of the design parameters in the development remained the same. The second mini UAV was then made with a name, Soaring Eagle.

Nevertheless, it is sad to say that while hunting for a take-off weight on the computing progression, the design process did not converge. A value of weight that made $\Delta$ the smallest was assigned to be the take-off weight. Note that here $\Delta$ is the difference between logarithms of the guessed empty weight and the calculated one based on previous aircraft of the same kind.[2] More unhappily, Soaring Eagle crashed at the first flight trial, was later fixed but crashed again at the contest. Since the mission was incomplete, no way to say it meets the requirement.

Next two UAVs were to challenge a payload requisite of 19.8 pounds. On the other hand, to improve the convergence of the design process, all mini UAVs including foreign ones and participants' were put together to obtain a new regression line and this did work, a solution of take-off weight appeared. In the spring of Year 2009, these two UAVs, TYLL-H and TYLL-L, rolled out. The TYLL-H was with high wing and TYLL-L the low. To satisfy the requirements of increasing payloads, the third author recommended students reduce the empty weight, especially the horizontal tail weight. These two vehicles were going to use the smaller horizontal tails than those of One-Piece and Soaring Eagle. Even with the satisfactory longitudinal stability of the forerunners' and no need to modify the horizontal tail too much, the longitudinal x-plot was still applied to see if it worked or not with the larger wings. Anyway, these two aerial vehicles did not bring to us too much excitement because TYLL-L crashed and TYLL-H obtained only 5$^{th}$ place although it carried 21.56 pounds for its shipment (actually, it reaches the goal).

For those four mini UAVs, airplane aerodynamics (not calibrated for Reynolds number effect) was temporarily used, and it showed not much discrepancy between the analysis and flight test results. This is probably by that the order of Reynolds numbers drops from six to five, aerodynamic characteristics did decrease but not very much. For the sake of pursuing precision, recent work will use low Reynolds number aerodynamics. Also, note that both two vehicles with low wing were all destroyed in the flight competition; the causes are worth finding out. So far, it would be blamed that we did not make lateral stability analysis (even without any directional x-plot). New design will cover this subject anyway. Table 2 lists all previous and recent work of our group in brief.

In the spring of 2010, an air vehicle designed by this adapting airplane sizing method named as Devil Bat was fabricated. It has an unusual shape, three surfaces. While tested on the first time, Devil Bat was a brand new plane for the third author to fly. It was not an easy task because he was used to the conventional configurations. It did not successfully lift-off but sat on the ground with damage to engine mount probably due to unexpected fast pitch up motion. During the following days, Chang[*] and his classmates were busy doing the repeated work preparing for flight tests, including that to fix the damaged air vehicle almost after every trial. Although the final test flight was a nearly perfect one, the ground controller felt that it was still not very handy to fly this three-surface stuff. Despite plenty of time being needed to get used to it, the time was running out. On the right next day, we went south for the competition.

---

[*]Yuan-Zun Chang, Designer of "Devil Bat," Student of Class 2010.

In the morning of that contest day, the lowest-fuel-consumption race went first so the third author flew Devil Bat with a low power. Moreover, this made him unable to recover it when he found that it would be out of bound in the landing phase of the second flight. Not very late after it was aloft, the host kept alerting the audience, by a loud speaker, to always stare at Devil Bat in the air. He was hinting that it might crash. Actually, it did and ruining most of its components. Students sacrificed their luncheon time repairing the damaged competitor and went just in time for the maximum-payload race in the afternoon.

Whilst preparing for take-off, one of the umpires warned the third author if he did not land Devil Bat on the designated landing zone, the team would be suspended. Under this kind of pressure, of course, he could not fly it very happily. Still, the approach looked good. However, with an unknown cause, it suddenly rolled down to the slope of bank, as happened in the first flight, out of bound. That umpire kept his words so Devil Bat was out and having no chance to see if it can get to the design goal even with then just minor damage, which could be fixed within decades of minutes. The second author doubts the roll be due to the sideward vortices induced by lateral head wind in the ground effect. Anyway, it really makes us feel upset that (the organizer) using a bank as the contest site without hanging a windsock to indicate the head wind direction.

The designer, Chang, and the second author always have the confidence in that Devil Bat can achieve its goal because the results of analysis illustrate it. After all, the lesson we should learn is that we must give the test-pilot lots of time to be used to the new design especially when an unconventional configuration unveils. This is probably analog to development of a new airplane.

Table 2 Listing of the Contestant Mini UAVs in NDU, TAIWAN (Weights in Pounds).

| Year | Name | $W_{TO}$ | $W_E$ | Payload, designed. | Payload, actual. | Ranking in the contest | Design Outlines | Notes |
|---|---|---|---|---|---|---|---|---|
| 2007 | One-Piece | 26.69 | 11.93 (Calculated), 11.35 (Contest) | 13.23 | 15.10 | 1st | Airplane Aerodynamics ($R_N$ of O (6) or greater). NACA 2412 Used for Design Calculation While G329 Actually Fabricated. Newly Designated Mission Specification and Mission Profile. Correction of Empty Weight for Balsa Wood from Varied Constructive Materials. | Conventional Configuration |
| 2008 | Soaring Eagle | 25.53 | 9.53 (Calculated), 10.24 (In Final Report) | 15 | — | Crashed | Low Wing | Conventional Configuration. The Design Process Did Not Converge. |
| 2009 | TYLL-H | 33.27 | 12.29 (Calculated), 14.99 (Contest) | 19.8 | 21.56 | 5th | Wing Apex Determined by Longitudinal X-plot. High Wing. | Conventional Configuration |
| 2009 | TYLL-L | 33.27 | 12.29 (Calculated), 13.43 (Contest) | 19.8 | 15.72 | 6th & Crashed at 2nd Trial with Payload | Wing Apex Determined by Longitudinal X-plot. Low Wing. | Conventional Configuration |
| 2010 | Devil Bat | 35.82 | 13.16 (Calculated), 15.07 (Contest) | 22 | 12.5 (Last Test Flight), 9.8 (Contest). | Landing out of Bound Three Times, Dismissed. | Three-surface Longitudinal X-plot Used for Canard and V-Tail Sizing and Wing Apex Position | Push Type Propulsion with Canard and V-tail. |
| 2010 | Monk Vulture | N/A | N/A | N/A | Not Flight-tested Yet | Not for Competition | Airfoil Maximum Lift Coefficient of Reynolds Numbers of Order of 5. Wing Moved Rearward to Have More Space to Carry Payloads. | In Master Degree Thesis for Research Purpose Only. |

## VII. Characteristics of This Group's Competitors

Details of some key points mentioned above are described in this section. Table 3 displays the sequence of development of adoption to mini UAV sizing from airplane design methodology. Beyond with this table to give the overall views, some of the interesting characteristics of our competitors will be explained individually in their own sub-sections followed.

Table 3 Characteristics of Mini UAVs in NDU, TAIWAN

| | | | 2007 One-Piece | 2008 Soaring Eagle | 2009 TYLL-H | 2009 TYLL-L | 2010 Devil Bat | 2010 Monk Vulture |
|---|---|---|---|---|---|---|---|---|
| a. Weight Trend | 1) International Mini UAVs | | ● | | | | | |
| | 2) Domestic Competing Mini UAVs (TAIWAN) | | | ● | | | | |
| | 3) Combining Internationals' and Domestics' | | | | ● | ● | | |
| | 4) Our Group's | | | | | | ● | ● |
| b. Fuel-Fraction Method with Roskam's Suggested Values | | | ● | ● | ● | ● | ● | ● |
| c. Weight Estimation with Reduction Factor of 0.442 to Compensation for Wood | | | ● | ● | ● | ● | ● | ● |
| d. C.G. Location of Major Components | 1) Roskam's Suggested Values | | ● | ● | ● | ● | ● | |
| | 2) Based on Measured Values of TYLL-L | | | | | | | ● |
| e. Performance Match Graph | 1) Sizing to FAR 23 Take-off Distance Requirements | | ● | ● | ● | ● | ● | ● |
| | 2) Sizing to FAR 23 Landing Distance Requirements | | ● | ● | ● | ● | ● | ● |
| | 3) Sizing to Others: Time to Climb, Rate of Climb. | | ● | | | | | |
| f. Aerodynamics: Maximum Lift Coefficients | 1) Airfoils | ① NACA's or G329 with $R_N$ of O(6) or greater | ● | ● | ● | ● | | |
| | | ② Experimental Vales with $R_N$ of O(5) | | | | | ● | ● |
| | 2) Eq. (4) | ① Assumed it can be applied. | ● | | | | ● | |
| | | ② Applied After Experimental Validations | | | | | | ● |
| g. Wing Planform Decision and Fuselage Sizing | 1) Based on Single Engine Propeller Driven Airplanes | | ● | | | | | |
| | 2) Previous Data of Our Earlier Mini UAVs | | ● | ● | ● | ● | ● | ● |
| h. Empennage Sizing | 1) The V-bar Methods | ① Based on Single Engine Propeller Driven Airplanes | ● | ● | | | | |
| | | ② Previous Data of Our Earlier Mini UAVs | | | ● | ● | | |
| | 2) Combined 1) With Longitudinal X-plot | | | | | | ● | ● |
| i. Preliminary Stability Analysis | 1) Static Longitudinal X-plot | ① Airplane Aerodynamics | – | – | ● | ● | | |
| | | ② Low Reynolds Number Aerodynamics | | | | | ● | ● |
| | 2) Static Directional X-plot | ① Airplane Aerodynamics | – | – | – | – | | |
| | | ② Low Reynolds Number Aerodynamics | | | | | ● | ● |
| j. Convergence of Weight Estimation | | | ● | No | ● | ● | ● | ● |
| k. Successful Flight Trials Before Contest | | | ● | | ● | ● | ● | No Need |
| l. Payload Goals Attained | | | ● | No | ● | No | No | Not Ready Yet To Test |

### A. One-Piece

The student designer of Class 2007, Cheng,[*] contributes to this group with the following: First trial of using mission specification and mission profile to estimate take-off weight, First one to apply the performance marching plot for mini-UAV, and, the most significant contribution, Setting-up the value of reduction factor for wood in subsequent applications of this team. The concept of weight reduction is from Ref. 2, which suggests a value of 0.75 for $W_{comp}$ / $W_{al}$, in which, $W_{comp}$ and $W_{al}$ are the weights of major components made of composites and aluminum, respectively. In One-Piece, a value of 0.69 was used. Then, with some measured components' weight, a value of 0.64 was applied for weight reduction further from composite to balsa wood, that is, $W_{wood}$ / $W_{comp}$ was set to be 0.64. Here, $W_{wood}$ is the weight of component made of wood. The net factor, $W_{wood}$ / $W_{al}$, is therefore 0.69 x 0.64, which is, 0.442. The calculated empty weight subtracting weights of non-wooden components was multiplied by this number, 0.442. In One-Piece, the engine with 1.323 pounds, landing gears with 1.543 pounds, and the fixed

[*]Po-Yu Cheng, in His Final Report of "One-Piece" Design, Written in Traditional Chinese, May 2007.

equipment with 1.102 pounds are considered as the non-wooden components. By adding these weights back to the above product, the reduced empty weight is obtained. As shown in Fig. 5 for the later usage, compared with the measured weights in the contests, this correction method works fair for all our competing vehicles.

### B. Soaring Eagle

Although he did not succeed in the competition, the designer of Class 2008, Chiang,* still has his role in this study. He was assigned by the second author to use the weight database of Years 2006 and 2007 contestants. As shown in Group 2 of Table 4, the value of A is greater than B compared with others in which with all As being less than Bs. Probably owing to this strange phenomenon, he suffered with the difficulty of no solution for his weight estimation as shown in Fig. 6. Note that the pair of curves of One-Piece that has a solution is also depicted. The reason why Soaring Eagle has no intercept point is still unclear. The second author doubts that it could be the great discrepancy of fabrication skills among the competing college student teams. However, this suspicion could be nonsense. The consistence in the fabricating skills of Mini UAVs in Group 1 of Table 4 cannot be expected but the corresponding trend works.

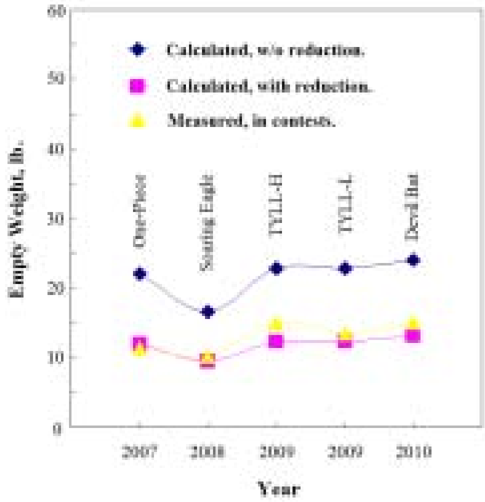


**Figure 5. Empty Weight Reduction for Balsa Wood.** *By using the reduction factor of 0.442 to reduce weight for wood from metals, this figure shows an adequate result for all competing vehicles.*

The suspicion did say something. The first author suggested Lu† to combine both the international (Group 1) and domestic (Group 2) plus new data of Year 2008's to form the weight trend and it works for next two designs, TYLL-H and TYLL-L. Note that all mini UAVs in Group 1 of Table 4 were made by professional technicians and the domestic vehicles in Groups 2 and 3 were made only by college students in Taiwan.

To remove this uncertainty, we started to form the weight trend for our own team, Groups 4 and 5 in Table 4, and it is working very well. Therefore, the lesson we have so far would be that the reliable beginning for weight estimation of mini UAVs is the formation of individual trend line based on the group's own database.

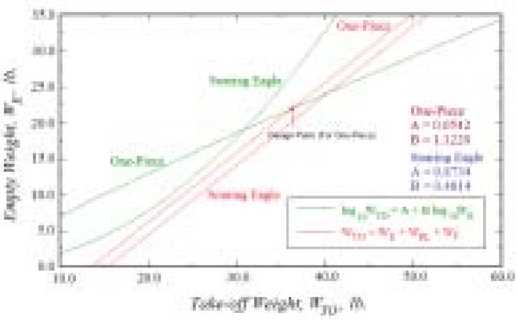


**Figure 6. Weight Estimation (One-Piece and Soaring Eagle).** *The weight trend line (green) cannot cut the empty weight line (red) found by fuel-fraction method in "Soaring Eagle" case, while there is an intersection in "One-Piece" case.*

Table 4 Weight Trend Equations

| $log_{10}W_{TO} = A + B\ log_{10}W_E$ (Ref. 2) | A | B |
|---|---|---|
| 1. International Mini-UAVs: Buster, Dragon Eye, Evolution, Javelin, Pointer FQM-151A, Puma, Raven RQ-11, Scorpio 6, Skylark, Snipe MK 15, Tracker, Wasp. | 0.0542 | 1.122 |
| 2. Domestic Mini-UAVs: NDU (Y2006), One-Piece, TKU (Y2006), AFIT (Y2007), NCKU (Y2007), AFA (Y2007), YDIT (Y2007). | 0.8734 | 0.4814 |
| 3. Combination of Groups 1, 2 and the following: Soaring Eagle, AFA (Y2008), NCKU-1 (Y2008), NCKU-2 (Y2008), ITB (Indonesia, Y2008). | 0.1306 | 1.1139 |
| 4. Our Group（Including 3 UAVs Belong to Beginners' Level）: NDU (Y2006), One-Piece, Soaring Eagle, TYLL-H, TYLL-L, NDU (Y2009-Beginner), AAROC-1 (Y2009-Beginner), AAROC-2 (Y2009-Beginner). | 0.5193 | 0.8418 |
| 5. Our Group (Advanced Level Only): NDU (Y2006), One-Piece, Soaring Eagle, TYLL-H, TYLL-L. | 0.1042 | 1.2767 |

*Chorng-Ming Chiang, in His Final Report of "Soaring Eagle" Design, Written in Traditional Chinese, March 2008.
†Yuh-Chuan Lu, Designer of "TYLL-H" and "TYLL-L," Student of Class 2009.

**C. TYLL-H**

Each year tough competing teams showed their capacity to carry more and it brought us the urgent need to new requirement of increasing the payload. However, the third author asked students not to increase the empty weigh too much by keeping the horizontal tail about the same as the previous designs. Even that, the wing area must be enlarged to provide sufficient lifting force to bring more dead weights in the air.

As mentioned above, the longitudinal X-plot would be a good tool to do primary stability analysis for mini UAVs. Its original purpose is to find a suitable size for the horizontal tail to fit the requirement of S.M. of –10%. In this case, although not much choice could be made about the size of horizontal tail, Lu was still asked to use the longitudinal X-plot to find S.M. with the almost given horizontal tail area. He is actually the first person to use this tool for a mini UAV design.

Unfortunately, he was stuck with a strange result as shown in Fig. 7. Due to the tight schedule, the fabrication process could not stop there waiting him get through this problem. Therefore, the third author used his model-airplane experience to decide the position of wing apex and kept the process going. Finally, after study, the second author found that the key parameter is the x-coordinates of the wing apex. With an inappropriate number for this parameter, people cannot find a suitable design for mini UAV. See Figs. 7 and 8 for this concept.

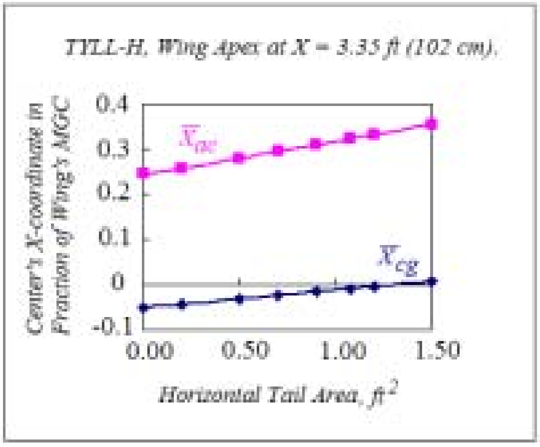


**Figure 7. Longitudinal X-plot for TYLL-H with Wing Apex at 3.35 ft (102 cm).** *Within the assigned range of horizontal tail areas, a neutral point does not exist; the designer cannot have the chance to turn his (or her) design from instability to stability by increasing the horizontal tail area. It is a poor design.*

The conclusion we have from this coincidence are: 1) Longitudinal X-plot works for mini UAV design even in this case the airplane aerodynamics rather than that of low Reynolds number was used. If not, we certainly would have no chance to find this new parameter. 2) Model-airplane experience can yet play the dominant and undeniable role in racing Taiwanese mini UAVs. That is why other teams without knowing exactly the mini UAV design method like us can still win the first prize.

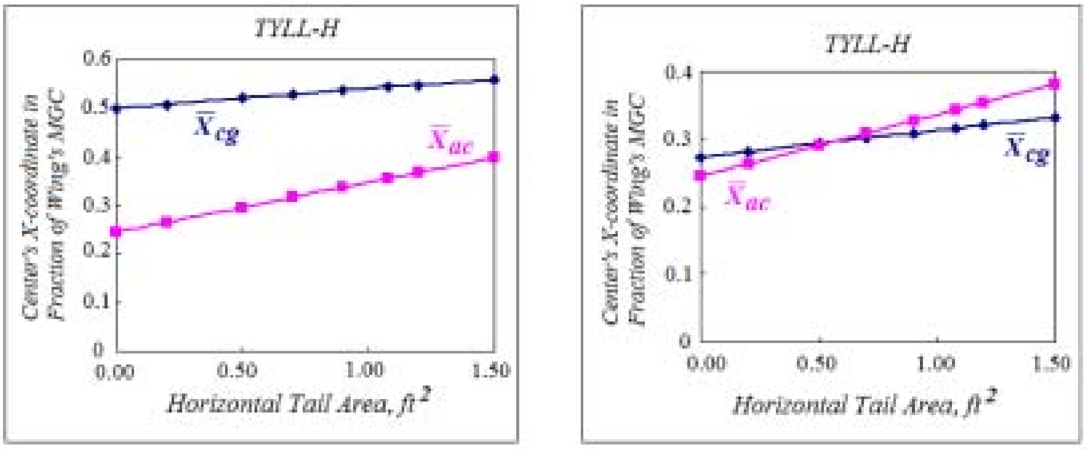


*a) Wing Apex, X = 2.62 ft (80 cm).* *b) Wing Apex, X = 2.92 ft (89 cm).*

**Figure 8. Longitudinal X-plots for TYLL-H.** *a) If the wing apex is placed at x = 2.62 ft (80 cm), it is still a poor layout. b) For the wing apex at x = 2.92 ft (89 cm), it turns out be a better design since the neutral point appears. The actual x-coordinate of the wing apex for TYLL-H after fabrication is 2.97 ft (90.5 cm). The origin of x-axis is set at 1.64 ft (50 cm) ahead of the fuselage apex.*

### D. TYLL-L

Lu and his teammates fabricated two air vehicles, TYLL-H and TYLL-L. The TYLL-L was supposed to have lower directional stability. Without any directional stability analysis, we will never know it is correct or not. The major parameters that affect the directional stability are: fuselage, vertical tail, propeller effect, and the minor ones: wing sweep angle and dihedral angle. If work that is more precise is demanding, cross effect should be kept into consideration. However, for primary stability analysis, expecting $C_{n_\beta}$ to have the number as shown in Eq. (6) is enough.

### E. Devil Bat

The adaptation of airplane sizing methodology to our mini UAVs was almost developed just before Chang[*] designed his "Devil Bat." He came to us with a rough draft having a tractor-type engine, a straight wing and a vee-tail. The third author assigned him to use a pusher-type engine. A canard was probably necessary if payload goes up to 22 lb. (10 kg), according to the second author. Chang at that time had an unusual pattern, i.e., three-surface configuration to work with.

He followed the design process discussed in Fig. 1 and adoption keys shown in Figs. 2-4[†] to fulfill his job and fully got to the point to show the characteristics of mini UAV different to those of airplanes. For weight trend, the Group 4 (Table 4) was used. For airfoils working at Reynolds number range of $10^5$-$10^6$, NACA 66 was selected with the experimental data to give section maximum lift coefficient of 1.0 at $R_N$ = 4.06 x $10^5$ from Ref. 10. Rather than the $\bar{V}$ method, the three-surface longitudinal X-plot was applied since he was go to use the canard and V-tail layout. The effect of thrust line of pusher type engine on pitching moment coefficient was also evaluated.

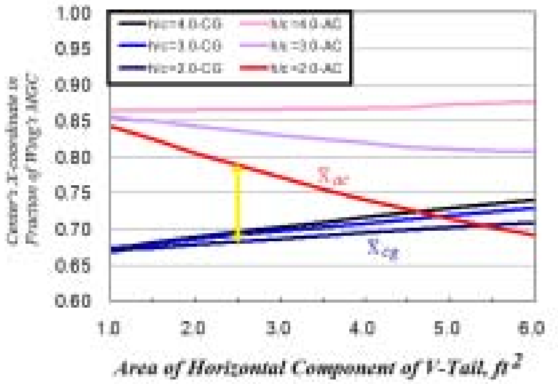


**Figure 9. Longitudinal X-Plot for Three-Surface Configuration (Devil Bat).** *By keeping area ratio, h/c, with 2.0, there is a chance for instability to happen to be stable with the area of V-tail decreasing. (Copied from Yuan-Zun Chang, Final Report of "Devil Bat," March 2010)*

The achievements of Devil Bat are as following: 1) First mini UAV with unconventional configurations designed by the adapted airplane sizing method developed by this study. 2) First mini UAV using three-surface longitudinal X-plot to determine the areas of canard and V-tail simultaneously. 3) First mini UAV to take the power effect on longitudinal stability into consideration during the conceptual design phase. Figure 9 shows the three-surface longitudinal X-plot of Devil Bat. In this figure, h/c means $S_h/S_c$, and $S_c$ is the area of canard and $S_h$ the area of horizontal component of V-tail. The ratio of $S_h/S_c$ of 2 was chosen to hold Eq. (5) and this made V-tail area become 2.942 ft$^2$ (2737 cm$^2$). The dihedral angle of V-tail was chosen to be 30 degrees.

### F. Monk Vulture

This uninhabited air vehicle is designed to search for the maximum amount of payloads that it, or all competitors, can carry using the piston engine with 2.8 hp at 15000 rpm assigned by the organizer. The proposed solution is that by moving the wing afterward on the fuselage of "TYLL-L," to have larger fuselage space to carry more dead weights. In order to acquaint enough lift at take-off, a canard is probably needed.

Toward the end of his research work for degree of mater of science, the fourth author has already achieved the accomplishments described below. Equation (4) was validated by using a set of experimental data from Wu's[‡] work. Wind tunnel testing was conducted to two sets of wing models at $R_N$ = 1.6 x $10^5$. Each set has two wing models with the same aspect ratio. One model is with endplates on both tips, the other none. Table 5 shows the results of evaluation. It is then clear that Eq. (4) can be applied for Monk Vulture.

[*] Yuan-Zun Chang, See Section VI.
[†] Validation of Eq. (4) Not Included.
[‡] Chang-Chieh Wu, See Sub-section D in Section V.

Another purpose of Monk Vulture is to use the fuselage of TYLL-L and modify its vertical tail to give sufficient directional stability according to Eq. (6). The primary directional stability analysis using the original data of TYLL-L shows that $C_{n_\beta}$ for TYLL-L is 0.0007 per degree (Fig. 10). This implies that we need to make the vertical tail bigger. Monk vulture still keeps its engine at the head and a possible three-surface configuration will be applied. Unlike Devil Bat, the power effect on the longitudinal stability in Monk Vulture could be negligible but the slipstream effect of propeller on the canard should not be forgotten. Before this manuscript is completed, Monk Vulture is still being fabricated.

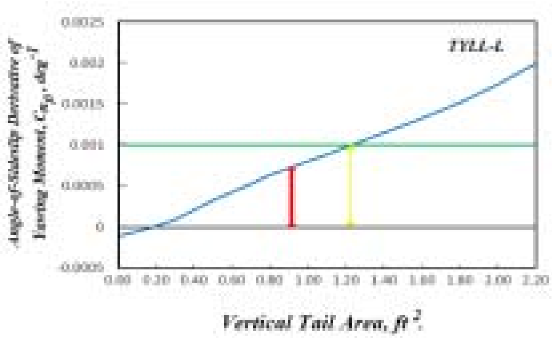


**Figure 10. Directional X-Plot for TYLL-L.** *As shown in this figure, TYLL-L possesses a lower directional stability as Eq. (6) says (Red). To obtain that high, need to make a VT area enlargement (Yellow).*

Table 5 Validation of Eq. (4)

| | NACA 0012 | GÖETTINGEN 329 |
|---|---|---|
| $R_N$ | 1.6 x $10^5$ | 1.6 x $10^5$ |
| Model Aspect Ratio | 7.56 | 8.50 |
| Model Taper Ratio | 1 | 1 |
| $k_\lambda$ | 0.88 | 0.88 |
| Experimental $c_{l_{max}}$ * | 1.05 | 1.30 |
| $c_{l_{max_r}} + c_{l_{max_t}}$ † | 2.10 | 2.60 |
| $k_\lambda(c_{l_{maxr}} + c_{l_{maxt}})/2$ ‡ | 0.924 | 1.14 |
| Experimental $C_{L_{max}}$ * | 0.99 | 1.27 |
| Discrepancy | 6.67% | 10.2% |

* Chang-Chieh Wu, See Sub-section D in Section V.
† In this case, $\lambda = 1$, the root and tip airfoils are the same.
‡ See Ref. 4.

## VIII. Configurations of Mini UAVs in NDU, TAIWAN

Now, it is interesting to reveal all of our air vehicles. As shown in Fig. 11, the four mini UAVs with conventional configurations, One-Piece, Soaring Eagle, TYLL-H, and TYLL-L, are placed together to display how they look like. Accompanying is Table 6 to demonstrate the comparison of their shapes. The two recent mini UAVs using the now developed method, Devil Bat and Monk Vulture, are put on view respectively in Figs. 12 and 13. Their individual sizes are also shown in Table 6.

## IX. Mini UAV Sizing Method

At this moment, it is good to give a systematic summary[*] for mini UAV sizing against a payload requirement before further discussion is made. (We sincerely expect that it can be extended to other requirements as many as possible in the future.) With Fig. 1, these steps are:

Step 1. Build a mission profile from the mission specification issued by the Competition, in this case, the payload requirement dominates. For each team, construct its own weight trend line for the previous competing mini UAVs.

Step 2. Use the fuel-fraction method[2] to estimate the mission fuel weight after a guess of take-off weight is made first. For cruise phase, Breguet's range equation with a measured fuel consumption rate is adequate. For other mission phases (loiter phase not included), do as suggested in Ref. 2. Obtain a tentative empty weight.

Step 3. With the guessed take-off weight, find the allowable value of empty weight from this line.

Step 4. Compare the values for tentative empty weight and for allowable empty weight. If they do not match within the tolerance pre-selected, guess a new take-off weight and repeat Steps 2 to 4.

Step 5. Do weight reduction by using 0.442 as described in Sub-section A of Section VII. Other teams might need different numbers for their own weight reduction factors.

Step 6. Break the take-off weight into component weights according to the weight fractions of existing previous air vehicles. In our case, the data of One-Piece ran first for modeling and more is available when time keeps going.

Step 7. Carry out the sizing calculations to take-off and landing distance requirements with the methods in Ref. 2. Consider all mini UAVs as FAR 23 airplanes.

[*]We hope anyone who wants to participate in the contest will find it benefit to follow these guidelines to get better scores for his (her) report, at least, good to a Taiwanese contestant.

Step 8. Construct a performance matching plot only for take-off and landing distance requirements in this type of vehicles. Draw a horizontal line on the graph with a known power loading, which is the ratio of the reduced take-off weight to the given horsepower assigned by the organizer. Along this horizontal line, select a design point as close as possible to the intersection cut with the take-off distance-sizing curve.

Step 9. Determine from the design point: take-off wing loading, take-off power loading, maximum lift coefficients (take-off and landing), wing aspect ratio and wing area.

Step 10. Perform Steps 1-9 of Preliminary Design Sequence I in Ref. 4. While selecting the suitable airfoils, using the experimental aerodynamic data with low Reynolds numbers in the range of 1 x $10^5$ to 1 x $10^6$ is strongly recommended. Some simulation software packages might be good to create the airfoils but errors could be introduced in their lift coefficients. Note that Eqs. (3) and (4) in Section V still apply. On the other hand, procedures are adjusted to fit the special circumstances for this type of rival mini UAVs, for example, no need to do selection of propulsion in its Step 5 (Ref. 4) since it is already assigned to be one piston engine having 2.8 hp.

Step 11. Draw the proposed configuration to scale. With C.G. locations based first on the suggested values in Ref. 4, or more in reality, the measured data of previous vehicles, then, do the weight and balance analysis.

Step 12. Construct the longitudinal X-plot and the directional X-plot.

Step 13. Follow the guidelines in Chapter 12 of Ref. 4 to do a Class I drag polar analysis.

Step 14. Perform Steps 13-16 of Preliminary Design Sequence I in Ref. 4 to complete mini UAV sizing for contest. Note that details of "sizing iteration and re-configuration" in Fig. 1 can be found in these steps (Ref. 4).

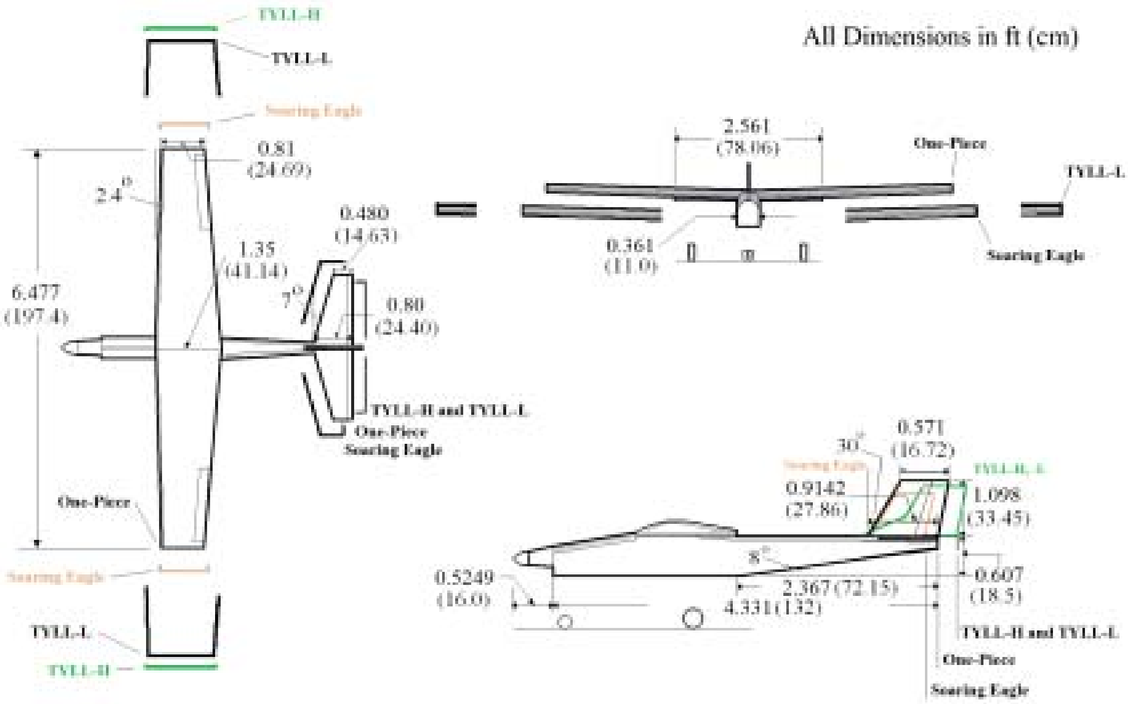


**Figure 11. Three Views of Conventional Configurations (One-Piece, Soaring Eagle, TYLL-H, and TYLL-L).** *Shown is the size-comparison of their wings, horizontal tails, and vertical tails. The base views with dimensions are for "One-Piece."*


**Figure 12. Devil Bat.** *As the first mini uninhabited aerial vehicle with three-surface configuration designed by the adapted airplane sizing method, Devil Bat has the canard, V-tail, high wing, and the pusher-type engine. (Copied from Yuan-Zun Chang's final report with his permission.)*

**Figure 13. Monk Vulture (Proposed Configuration).** *To improve directional stability of TYLL-L and to carry more payloads, Monk Vulture has a similar shape, but with a canard, compared with TYLL-L. This mini UAV is a traction-type engine propeller-driven air vehicle.*

Table 6 Geometric Data of Mini UAVs in NDU, TAIWAN [Dimensions are in ft (cm), or $ft^2$ ($cm^2$).]

| | | 2007 One-Piece | 2008 Soaring Eagle | 2009 TYLL-H | 2009 TYLL-L | 2010 Monk Vulture | 2010 Devil Bat | |
|---|---|---|---|---|---|---|---|---|
| Fuselage | Length | 4.856 (148) | 4.692 (143) | 5.085 (155) | 5.085 (155) | 5.085 (155) | 5.741 (175) | |
| | Max. Width | 0.3609 (11) | 0.3609 (11) | 0.4265 (13) | 0.4265 (13) | 0.4265 (13) | 0.4462 (13.6) | |
| | Max. Height | 0.6070 (18.5) | 0.4921 (15) | 0.6562 (20) | 0.6562 (20) | 0.6562 (20) | 0.6562 (20) | |
| Wing | Wing Area | 6.993 (6497) | 8.500 (7897) | 13.15 (12238) | 12.53 (11642) | 12.52 (11631) | 12.65 (11752) | |
| | Wing Span | 6.477 (196.3) | 7.218 (220) | 10.35 (315.4) | 9.92 (302.4) | 9.92 (302.4) | 9.678 (295) | |
| | Wing MGC | 1.102 (33.60) | 1.27 (38.6) | 1.286 (39.2) | 1.276 (38.9) | 1.28 (39.0) | 1.312 (40) | |
| | Aspect Ratio | 6 | 7 | 8 | 8 | 7.84 | 7.4 | |
| | Taper Ratio | 0.6 | 0.56 | 0.71 | 0.71 | 0.70 | 0.7 | |
| | Sweep Angle of Quarter Chord | 0 | 0 | $1.8^o$ | $1.8^o$ | $1.8^o$ | $1.64^o$ | |
| | Dihedral Angle | $2^o$ | $5^o$ | $2^o$ | $2^o$ | $2^o$ | 0 | |
| | Wing Type | High Wing | Low Wing | High Wing | Low Wing | Low Wing | High Wing | |
| | Airfoil | Gott. 329 | Gott. 329 | NACA 66 | NACA 66 | Gott. 329 | NACA 66 | |
| Horizontal Tail | Hor. Tail Area | 1.64 (1524) | 2.4 (2230) | 1.08 (1006) | 1.08 (1006) | 1.65 (1528) | Vee Tail | 2.942 (2737) |
| | $S_e/S_h$ | 0.545 | 0.5 | — | — | — | | — |
| | $x_h$ | 2.820 (86) | 2.822 (86) | 2.93 (89.3) | 2.93 (89.3) | — | | — |
| | $V_h$ bar | 0.6 | 0.627 | 0.475 | 0.395 | — | | — |
| | Span, $b_h$ | 2.561 (78.1) | 3.1 (94) | 2.296 (70) | 2.296 (70) | 2.289(69.8) | | 3.6 (109.8) |
| | Aspect Ratio | 4.0 | 4.0 | 4.87 | 4.87 | 3.19 | | 4.6 |
| | Taper Ratio | 0.6 | 0.45 | 0.52 | 0.52 | 0.65 | | 0.6 |
| | Sweep Angle of Leading Edge | $7^o$ | $7^o$ | $14.7^o$ | $14.7^o$ | $14.7^o$ | | $17^o$ |
| | Airfoil | Flat Plate | Flat Plate | Flat Plate | Flat Plate | NACA 0012 | | Flat Plate |
| Vertical Tail | Ver. Tail Area | 0.8031 (746) | 0.517 (480) | 0.94 (873.3) | 0.94 (873.3) | 1.2 (1115) | Canard | 1.25 (1163) |
| | $S_r/S_v$ | 0.413 | 0.45 | — | — | — | | — |
| | $x_v$ | 2.820 (86) | 2.657 (81) | 2.93 (89.3) | 2.93 (89.3) | — | | — |
| | $V_v$ bar | 0.05 | 0.0224 | 0.0202 | 0.0221 | — | | — |
| | Span, $b_v$ | 1.098 (33.45) | 0.79 (24.0) | 0.98 (29.87) | 0.98 (29.87) | 1.26 (38.5) | | 2.25 (68.58) |
| | Aspect Ratio | 1.5 | 1.5 | 1.5 | 1.5 | 1.33 | | 4.1 |
| | Taper Ratio | 0.6 | 0.45 | 0.33 | 0.33 | 0.49 | | 0.5 |
| | Sweep Angle of Leading Edge | $30^o$ | $30^o$ | $30^o$ | $30^o$ | $30^o$ | | $15^o$ |
| | Airfoil | Flat Plate | Flat Plate | Flat Plate | Flat Plate | NACA 0012 | | Flat Plate |

Table 6 (Cont'd) Geometric Data of Mini UAVs [Dimensions are in ft (cm), or $ft^2$ ($cm^2$).]

| *Monk Vulture* | Canard Area, $S_c$ | Span, $b_c$ | Area Ratio, $S_h/S_c$ | Aspect Ratio | Taper Ratio | Sweep Angle of Leading Edge | Airfoil |
|---|---|---|---|---|---|---|---|
| Canard | 0.90 (836.1) | 2.35 (71.6) | 1.8 | 6.09 | 0.67 | 7.3 $^o$ | NACA 0012 |

## X. Discussion

Devil Bat used Group 4, which includes all air vehicles belonging to this team, for its weight trend. The calculated empty weight without doing correction with the factor of 0.442 will be much greater than the measured value in the contest (Fig. 5). It seems to us a little bit frustrated that weight reduction is still needed since the weight trend of our own group was already applied (the manufacturing skill and construction materials almost the same). The reason why it occurs is shown in Table 7. Although Cruise Phase is the longest among all mission phases, fuel-consumption is strangely the least (by Ref. 11 with truncation). This is probably because fuel-fractions used in other phases, say, landing, are from inhabited air vehicles' and the unreasonableness appears while compared to that of the cruise phase. Therefore, new estimation is necessary and the possible solution might be in Ref. 3.

As shown in Table 5, Eq. (4) is validated with two airfoils in $R_N = 1.6 \times 10^5$. This value is close to the lower bound of range with $10^5$-$10^6$. It is with risk to say Eq. (4) is true for the whole range. It seems to us that more experimental airfoil data should be needed.

On site of competition, Devil Bat was aloft at the last challenge with a payload of 9.79 lb (4.45 kg) having a take-off ground round of 154 ft (47.0 m). The corresponding take-off parameter, $TOP_{23}$, is 18.32. In Page 95 of Ref. 2, according to its Eq. (3.4), we can calculate the related $S_{TOG}$, the take-off ground run, to be 92.8 ft (28.3 m). Compared with the measured value, it shows an inconsistency of 39.8 % in which doubt of mini UAVs being FAR 23 airplanes exists. Therefore, further check of this concept, "Regulating take-off distance of mini UAVs with FAR 23," is necessary. Alternatively, it might be sensible to establish a new relationship between $S_{TOG}$ and $TOP_{23}$ (then this take-off parameter would be re-named with the subscript deleted).

Table 7 Fuel Fraction and Weight for Each Phase (Devil Bat, Calculated by AAA 3.12[11])

| Mission Profile | Fuel Fraction | Fuel Weight, begin (lb.) | Fuel Consumed (lb.) |
|---|---|---|---|
| 1. Engine Start and Warm-up | 0.9980 | 1.3 | 0.1 |
| 2. Taxi | 0.9980 | 1.2 | 0.1 |
| 3. Take-off | 0.9980 | 1.1 | 0.1 |
| 4. Climb and Acceleration | 0.9950 | 1.0 | 0.2 |
| 5. Cruise | 0.9991 | 0.8 | 0.0 |
| 6. Descent | 0.9950 | 0.7 | 0.2 |
| 7. Landing, Taxi, and Shut-down | 0.9950 | 0.5 | 0.2 |

Almost all teams in the competition are hunting for the maximum payload they can bring in the air. If with only model airplane experience, what they can do for their "design" is simply by trial and error, build, fly, and crash. This is not the case here with the above-proposed methodology since we could demonstrate the direction about how to estimate it. However, owing to already seeing the demand of doing more improvement of the methods as discussion we made so far, the idea, yet the result, is shown here.

By comparing, the two red lines shown in Fig. 6 are parallels and that one with larger payload is on the right. By increasing payload, the weight-splitting line (red) will keep moving in parallel manner to the right. The design point, specifying the take-off wing loading in a matching graph, also the intersection between the weight-splitting line (red) and the trend line (green), will go upwards along the green line. That means the wing loading is decreasing since the design point is climbing to the left along the boarder line in the matching plot. Lower wing loading with the take-off weight being frozen in design implies that a bigger wing is necessary. Designers certainly cannot enlarge their wings without any limitation since the span has been specified by the contest. When wing area reaches its maximum by touching the restricted span, the take-off weight is not allowed to increase any more and the maximum payload will be found.

As told in the story of Section VI, Devil Bat went to challenge the lowest-fuel-consumption rate first in the competition but it was originally designed only for a payload requirement. An unexpected roll-to-right crash in the first flight and out-of-bound crash-landing in the second flight affected our activities in the coming maximum payload race. Failure in the main race might come from the wrong strategy we made before. If the organizer keeps the sequence of the flight contest in the future, we might consider adding an endurance, or loiter phase to the mission profile.

## XI. Conclusion

As described in the beginning, this study was motivated by teaching students for their competing aircraft. This paper is more like for educational purpose than for research. In order to work very well, development of sizing mini UAVs by airplane design methods is still progressing. However, students learn by practice designing their own aircraft and finally see them aloft or crashed depending on how well they prepare for the flights, including arrangement of schedule, communicating with the test-pilot, on-site repairs, and so on. All are beyond the course "Airplane Design" can teach them and good for their career. For teachers, the more we spend on it the more we find what to do in the future for mini UAV design.

From Section X, the following are probably worth doing in the future:

1) Use a new approach to estimate mission fuel weight with advantage of no need to do weight reduction since the weight trend is established from our group's own vehicles now.
2) If possible, conduct wind tunnel testing for low Reynolds number airfoils, covering a wider spectrum in the range of $10^5 < R_N < 10^6$.
3) Measure the take-off distances on site to establish a new equation relating them to the take-off parameters defined as in Eq. (1) but with revision. Use this equation to construct a new barrier for sizing to take-off requirement in the matching graph. (Or, another new approach to find relation of the take-off distance to wing loading and power loading at take-off.)
4) Develop the methodology for sizing to endurance requirements, or actually, it is to cruise speed requirements.
5) After finishing Item 3 above, estimate the maximum payload the assigned engine can drive and wait to see what will happen in the coming contests to evaluate this calculation.

## Appendix

The following acronyms are to explain the abbreviations we put in Table 4 (Group 1 not included): AFA (Air Force Academy, Taiwan), AFIT (Air Force Institute of Technology, Taiwan), AAROC (Army Academy, ROC, Taiwan), ITB (Institute Teknologi Bandung, Indonesia), NCKU (National Cheng Kung University), NDU (National Defense University), TKU (Tamkang University), TYLL-H (Tzeng, Yu, Lin, and Lu-all last names of teammates, with high wing; while TYLL-L with low wing), YDIT (Yung-Ta Institute of Technology).

## Acknowledgments

This work was supported in part by the National Science Council, Taiwan, ROC under NSC 98-2221-E-606-016. The authors are indebted to all undergraduates who participated in the contests and fabricated all the competing air vehicles. We also thank National Defense University, Taiwan, ROC and its faculty members directly and indirectly for their help to the studies.

## References

[1]Weibel, R. E. and Hansman, R. J. Jr., "Safety Considerations for Operation of Different Classes of UAVs in the NAS," presented at the AIAA 3rd "Unmanned Unlimited" Technical Conference, Workshop and Exhibit, Chicago, Illinois, Sept. 20-22, 2004.

[2]Roskam, J., *Airplane Design, Part I: Preliminary Sizing of Airplanes,* DARcorporation, Lawrence, KS, 2005.

[3]Raymer, D. P., *Aircraft Design: A Conceptual Approach*, 4th ed., AIAA Education Series, AIAA, Reston, VA, 2006.

[4]Roskam, J., *Airplane Design: Part II: Preliminary Configuration Design and Integration of the Propulsion System*, DARcorporation, Lawrence, KS, 2004.

[5]Nicolai, L. M., *Fundamentals of Aircraft Design,* University of Dayton, Dayton, OH, 1975.

[6]Roskam, J., *Airplane Design, Part VI: Preliminary Calculation of Aerodynamics, Thrust, and Power Characteristics,* DARcorporation, Lawrence, KS, 2004.

[7]Lissaman, P. B. S., "Low-Reynolds-Number Airfoils," *Annual Reviews of Fluid Mechanics*, Vol. 15, 1983, pp. 223-239.

[8]Anderson, J. D., Jr., "Airplane Design Methodology: Setting the Gold Standard," *AIAA Journal*, Vol. 44, No. 12, December 2006, pp. 2817-2819.

[9]Taylor, J. W. R., *Jane's All the World's Aircraft*, Jane's Publishing Company, London, UK, 2006.

[10]Rice, M. S., *Handbook of Airfoil Sections for Light Aircraft*, Aviation Publications, Appleton, WI, 1971.

[11]Advanced Aircraft Analysis, Version 3.12, DARcorporation, Lawrence, KS, 2006.

EVENT AGENDA

**AIAA Infotech@Aerospace 2010**

F

Adc

At A Glance | 20-Apr-2010 | 21-Apr-2010 | 22-Apr-2010 | All |

**Program For Thursday, 22-Apr-2010**

**Session 57- I@A-57** **Applications of Intelligent Propulsion Control I**
Chaired by: T. GUO and J. LITT, NASA Glenn Research Center, Cleveland, OH

| | | |
|---|---|---|
| 0900<br>AIAA-2010-3469<br>A Risk Assessment Architecture for Enhanced Engine Operation<br><br>J. Litt, L. Sharp and T. Guo, NASA Glenn Research Center, Cleveland, OH<br><br>SEE FIRST PAGE » | 0930<br>AIAA-2010-3470<br>Use of Propulsion Commands to Control Directional Stability of a Damaged Transport Aircraft<br><br>J. Urnes, The Boeing Company, St Louis, MO<br><br>SEE FIRST PAGE » | 1000<br>AIAA-2010-3471<br>Flight- Propulsion<br>Directional Stabilit<br><br>N. Nguyen and V.<br>Research Center,<br><br>SEE FIRST PAGE » |

**Session 58- I@A-58** **Control and Estimation Methods I**
Chaired by: V. STEPANYAN, NASA Ames Research Center, Moffett Field, CA

| | | |
|---|---|---|
| 0900<br>AIAA-2010-3472<br>Real- Time System Identification of a Small Multi- Engine Aircraft with Structural Damage<br><br>G. Chowdhary, W. DeBusk and E. Johnson, Georgia Institute of Technology, Atlanta, GA<br><br>SEE FIRST PAGE » | 0930<br>AIAA-2010-3473<br>Coordinated Control of a Team of Helicopters<br><br>M. Mattei, Second University of Naples, Aversa, Italy; and V. Scordamaglia, University of Reggio Calabria, Reggio Calabria, Italy<br><br>SEE FIRST PAGE » | 1000<br>AIAA-2010-3474<br>Stability Properties a<br>of the Control Allocat<br><br>Y. Yildiz, U. C. Santa<br>Kolmanovsky, Univer<br>Arbor, MI<br><br>SEE FIRST PAGE » |

**Session 59- I@A-59** **Enabling Plug and Play Systems I**
Chaired by: J. LYKE, U.S. Air Force Research Laboratory, Albuquerque, NM

| | | |
|---|---|---|
| 0900<br>AIAA-2010-3475<br>Appliqué Sensor Interface Module Based on 90nm Rad- Hard Structured Application-Specific Integrated Circuit<br><br>A. Vera, M. Sibley, and S. Ardalan, Micro-RDC, Albuquerque, NM; K. Avery and J. Lyke, U.S. Air Force Research Laboratory, Albuquerque, NM<br><br>SEE FIRST PAGE » | 0930<br>AIAA-2010-3476<br>Optical Networking for Aerospace Systems Provisioned Through Plug and Play Avionics<br><br>N. Francis, U.S. Air Force Research Laboratory, Albuquerque, NM; C. Collier, Science Applications International Corporation, Albuquerque, NM; K. Avery and J. Lyke, U.S. Air Force Research Laboratory, Albuquerque, NM<br><br>SEE FIRST PAGE » | 1000<br>AIAA-2010-34<br>Development<br>and- Play Avi<br><br>R. Vick, Scier<br>Corporation, /<br>U.S. Air Force<br>Albuquerque,<br><br>SEE FIRST PAGE |

**Session 60- I@A-60** **ISHM Software Tools I**
Chaired by: M. VENKATESH, General Atomics, San Diego, CA

| | |
|---|---|
| 0900<br>AIAA-2010-3478<br>Multiple Information Agents for Real- Time, ISHM: Architectures for Real- Time Warfighter Support<br><br>J. Crowder, Raytheon Company, Aurora, CO<br><br>SEE FIRST PAGE » | 0930<br>AIAA-2010-3499<br>Using the Integrated Vehicle Health Management Researc<br>to Identify Synergistic Test Opportunities<br><br>S. Koelfgen and J. Faber, NASA Dryden Flight Research (<br><br>SEE FIRST PAGE » |

**Session 61- I@A-61** **Situational Assessment Technologies III**

Chaired by: P. ZETOCHA, U.S. Air Force Research Laboratory, Albuquerque, NM, and C. TSCHAN, The Aerospace Corporatior

| | | |
|---|---|---|
| 0900<br>AIAA-2010-3481<br>Probabilistic Evidential Reasoning with Symbolic Argumentation for Space Situation Awareness<br><br>G. Takata and J. Gorman, Charles River Analytics, Cambridge, MA<br><br>SEE FIRST PAGE » | 0930<br>AIAA-2010-3482<br>Probabilistic Relational Models for Space Situational Awareness<br><br>A. Pfeffer, Charles River Analytics, Cambridge, MA<br><br>SEE FIRST PAGE » | 1000<br>AIAA-2010-3483<br>Data Driven Perfo<br>Process Managen<br><br>G. Haith and C. B<br><br>SEE FIRST PAGE » |

**Session 62- I@A-62** **Software Systems I**

Chaired by: J. MURPHY, NASA Ames Research Center, Moffett Field, CA

| | | |
|---|---|---|
| 0900<br>AIAA-2010-3484<br>Transitioning to Net- Centric Systems<br><br>F. Briggs, Wyle Aerospace Group, Lexington Park, MD<br><br>SEE FIRST PAGE » | 0930<br>AIAA-2010-3485<br>Migrating to a Product Line for Electronic Warfare Systems<br><br>S. Cohen, Software Engineering Institute, Pittsburgh, PA; D. Snelgrove, BAE, Hudson, NH<br><br>SEE FIRST PAGE » | 1000<br>AIAA-2010-3486<br>Analyzing Distributed Functions<br>Analysis<br><br>A. Morris, NASA Langley Rese<br>Massie, ARES Corporation, Ho<br><br>SEE FIRST PAGE » |

**Session 63- I@A-63** **Unmanned Aircraft System Platforms I**

Chaired by: G. PARKER, U.S. Air Force, Wright-Patterson AFB, OH

| | | |
|---|---|---|
| 0900<br>AIAA-2010-3487<br>Formation Control of Small Unmanned Air Vehicles Under Faulty Communications<br><br>T. Hino and T. Tsuchiya, University of Tokyo, Bunkyo-ku, Japan<br><br>SEE FIRST PAGE » | 0930<br>AIAA-2010-3488<br>Research Activity on Unmanned Air Vehicles at the University of Tokyo<br><br>T. Hino, M. Naruoka, and K. Miyaji, University of Tokyo, Bunkyo-ku, Japan; D. Kubo, Japan Aerospace Exploration Agency (JAXA), Mitaka-shi, Japan; T. Tsuchiya and S. Suzuki, University of Tokyo, Bunkyo-ku, Japan<br><br>SEE FIRST PAGE » | 1000<br>AIAA<br>First<br>Pilot<br>Platf<br><br>V. Jo<br>of Ka<br><br>SEE |

**1030 - 1100** **Networking Coffee Break**

**Session 64- I@A-64** **Applications of Intelligent Propulsion Control II**

Chaired by: T. GUO and J. LITT, NASA Glenn Research Center, Cleveland, OH

| | | |
|---|---|---|
| 1100<br>AIAA-2010-3490 | 1130<br>AIAA-2010-3491 | 120<br>AIA |

| | | |
|---|---|---|
| WITHDRAWN<br>Anti- Windup Design for a Vertical Tail Loss Transport Aircraft Using Differential Thrust<br><br>V. Stepanyan, Mission Critical Technologies, Inc., Moffett Field, CA; K. Kalmanje and N. Nguyen, NASA Ames Research Center, Moffett Field, CA<br><br>SEE FIRST PAGE » | Fast Engine Response for Emergency Aircraft Operation<br><br>W. Merrill, H. Tran Van, and G. Mink, Scientific Monitoring, Inc, Scottsdale, AZ; and J. Litt, NASA Glenn Research Center, Cleveland, OH<br><br>SEE FIRST PAGE » | Ada<br>Pres<br><br>C. C<br>Univ<br><br>SEE |

**Session 65- I@A-65** **Control and Estimation Methods II**

Chaired by: V. STEPANYAN, NASA Ames Research Center, Moffett Field, CA

| | | |
|---|---|---|
| 1100<br>AIAA-2010-3493<br>VCU Rotor- Wing Flight Control System<br><br>R. Demott, L. Mize and R. Klenke, Virginia Commonwealth University, Richmond, VA<br><br>SEE FIRST PAGE » | 1130<br>AIAA-2010-3494<br>Robust Attitude Control for Spacecraft Based on Normal Matrix and Pattern Search<br><br>H. Zhu, Beihang University, Beijing, China (prc)<br><br>SEE FIRST PAGE » | 1200<br>AIAA-2010-3495<br>Using an Autothrot<br>Saving Fuel on a F<br><br>R. Johnson, Iowa S<br><br>SEE FIRST PAGE » |

**Session 66- I@A-66** **Enabling Plug and Play Systems II**

Chaired by: J. LYKE, U.S. Air Force Research Laboratory, Albuquerque, NM

| | | |
|---|---|---|
| 1100<br>AIAA-2010-3496<br>The Space Plug- and- Play Avionics Common Data Dictionary - - Constructing the Language of SPA<br><br>D. Lanza and R. Vick, Science Applications International Corporation, Albuquerque, NM; J. Lyke, Air Force Research Laboratory, Kirtland AFB, NM<br><br>SEE FIRST PAGE » | 1130<br>AIAA-2010-3497<br>Cell- Based Architecture for Reconfigurable Wiring Manifolds<br><br>V. Murray and G. Feucht, University of New Mexico, Albuquerque, NM; J. Lyke, U. S. Air Force Research Laboratory, Albuquerque, NM; J. Plusquellic and M. Pattichis, University of New Mexico, Albuquerque, NM<br><br>SEE FIRST PAGE » | 1200<br>AIAA-2010-3549<br>Automatic Softw<br>Code from an xT<br><br>J. Christensen, S<br>Logan, UT; S. C<br>Logan, UT; B. H<br>Laboratory, Loga<br><br>SEE FIRST PAGE » |

**Session 67- I@A-67** **ISHM Software Tools II**

Chaired by: M. VENKATESH, General Atomics, San Diego, CA

| | |
|---|---|
| 1100<br>AIAA-2010-3498<br>Anomaly Detection Tool for ISHM<br><br>J. Schmalzel, NASA Stennis Space Center, Stennis Space Center, MS; M. Turowski and R. Franzl, Jacobs Technology, Stennis Space Center, MS; and F. Figueroa, NASA Stennis Space Center, Stennis Space Center, MS<br><br>SEE FIRST PAGE » | 1130<br>AIAA-2010-3500<br>HealthMAP – A M<br>Health Monitoring,<br><br>R. Kapadia and M.<br>Diego, CA<br><br>SEE FIRST PAGE » |

**Session 68- I@A-68** **Situational Assessment Technologies IV**

Chaired by: P. ZETOCHA, U.S. Air Force Research Laboratory, Albuquerque, NM, and C. TSCHAN, The Aerospace Corporatio

| | |
|---|---|
| 1100<br>AIAA-2010-3501<br>Engineering Resource Management Solutions by Leveraging Dual | 1130<br>AIAA-2010-3502<br>Statistical Methods for Correlating Space Environment Me |

| | |
|---|---|
| Data Fusion Solutions<br><br>C. Bowman, DF&NN, Broomfield, CO<br><br>SEE FIRST PAGE » | Amongst Multiple GEO Satellites<br><br>G. Haith and C. Bowman, DF&NN, Broomfield, CO; and C Corporation, Colorado Springs, CO<br><br>SEE FIRST PAGE » |

**Session 69- I@A-69** **Software Systems II**

Chaired by: J. MURPHY, NASA Ames Research Center, Moffett Field, CA

| | | |
|---|---|---|
| 1100<br>AIAA-2010-3503<br>Detecting Emergent Behaviors with Semi- Boolean Algebra<br><br>P. Haglich, Lockheed Martin Corporation, Arlington, VA; L. Pullum, Ridge National Laboratory, Oak Ridge, TN; and C. Rouff, Lockheed Martin Corporation, Arlington, VA<br><br>SEE FIRST PAGE » | 1130<br>AIAA-2010-3504<br>A Comparison and Evaluation of Real-Time Software Systems Modeling Languages<br><br>K. Evensen and K. Weiss, Jet Propulsion Laboratory, Padadena, CA<br><br>SEE FIRST PAGE » | 1200<br>AIAA-20<br>A New S<br>Undergr<br><br>L. Long<br>Pennsyl<br>Park, PA<br><br>SEE FIRS |

**Session 70- I@A-70** **Unmanned Aircraft System Platforms II**

Chaired by: G. PARKER, U.S. Air Force, Wright-Patterson AFB, OH

| | | |
|---|---|---|
| 1100<br>AIAA-2010-3506<br>Unmanned Aerial Vehicle Systems for Disaster Relief: Tornado Alley<br><br>W. DeBusk, Georgia Institute of Technology, Atlanta, GA<br><br>SEE FIRST PAGE » | 1130<br>AIAA-2010-3507<br>Study on Mini UAV Designs to Payload Requirements by Airplane Sizing Methodology<br><br>C. Hung, C. Lin, Y. Teng, C. Chang and Y. Wu, National Defense University, Tahsi, Taoyuan, Taiwan (roc)<br><br>SEE FIRST PAGE » | 1200<br>AIAA-2010-3508<br>Hardware Implementation of COTS Avionics S Vehicle Platforms<br><br>Y. Yeh and A. Ishihara, Carnegie Mellon Silic Kumar, Polytechnic Institute of New York Univ NASA Ames Research Center, Moffett Field,<br><br>SEE FIRST PAGE » |

**1230 - 1400** **Lunch**

**Session 71- I@A-71** **Applications Of Guidance, Navigation, & Control I**

Chaired by: D. ACCARDO, University of Naples "Federico II", Naples, Italy, and D. CLANCY, Lockheed Martin Corporation, Fort

| | | |
|---|---|---|
| 1400<br>AIAA-2010-3509<br>The Design of Rapidly Reconfigurable Filters for Attitude and Position Determination<br><br>R. Curry, M. Lizarraga, and G. Elkaim, University of California, Santa Cruz, Santa Cruz, CA<br><br>SEE FIRST PAGE » | 1430<br>AIAA-2010-3510<br>Autonomous Flight in GPS- Denied Environments Using Monocular Vision and Inertial Sensors<br><br>A. Wu and E. Johnson, Georgia Institute of Technology, Atlanta, GA<br><br>SEE FIRST PAGE » | 1500<br>AIAA-2010-3511<br>Magnetorquer Based Attitu Testplatform<br><br>D. Torczynski, Stanford Un Amini, Delft University of Te Netherlands<br><br>SEE FIRST PAGE » |

**Session 72- I@A-72** **Infotech R&D for Unmanned and Robotic Air Systems I**

Chaired by: M. FRANCIS, United Technologies Research Center, East Hartford, CT

| | | |
|---|---|---|
| 1400 | 1430 | 1500 |

| | | |
|---|---|---|
| AIAA-2010-3512<br>Evaluating the Performance of a UAS- Based Precision Agriculture Imaging Payload<br><br>D. Dvorak, J. Sorum, W. Semke, J. Neubert and R. Schultz, University of North Dakota, Grand Forks, ND<br><br>SEE FIRST PAGE » | AIAA-2010-3513<br>A First- Person View System for Remotely Operated Vehicles Using a Fisheye- Lens<br><br>P. Marine and O. Rawashdeh, Oakland University, Rochester, MI<br><br>SEE FIRST PAGE » | AIAA-2010-3514<br>Dispatch Interface f<br>Aerial Systems into<br><br>W. DeBusk, C. Brit<br>Georgia Institute of<br><br>SEE FIRST PAGE » |

**Session 73- I@A-73** **Intelligent Data Processing I**

Chaired by: R. SAVELY, NASA Johnson Space Center, Houston, TX

| | | |
|---|---|---|
| 1400<br>AIAA-2010-3515<br>Improved Submerged Inlet Conceptual Design Process Using Data Mining and Surrogate Modeling<br><br>F. Akram, M. Prior and D. Mavris, Georgia Institute of Technology, Atlanta, GA<br><br>SEE FIRST PAGE » | 1430<br>AIAA-2010-3516<br>An Event Detection Methodology for Identification of Aviation Mishap Leading Indicators<br><br>T. Marino and B. Fuller, Naval Surface Warfare Center, West Bethesda, MD | 1500<br>AIAA-2010-3517<br>Near Real- Time Optimal Prec<br>Aviation Data<br><br>R. Martin, NASA Ames Resea<br>and S. Das, University of Calif<br>CA<br><br>SEE FIRST PAGE » |

**Session 74- I@A-74** **Neural Network and Fuzzy Logic Methods I**

Chaired by: K. COHEN, University of Cincinnati, Cincinnati, OH

| | |
|---|---|
| 1400<br>AIAA-2010-3519<br>Flexible Object Architectures for Hybrid Neural Processing Systems<br><br>J. Crowder, Raytheon Company, Aurora, CO<br><br>SEE FIRST PAGE » | 1430<br>AIAA-2010-3520<br>Continuously Recombinant Genetic Neur<br><br>J. Crowder, Raytheon Company, Aurora,<br><br>SEE FIRST PAGE » |

**Session 75- I@A-75** **SDRE Approach for Robust Estimation and Control I**

Chaired by: Q. LAM, Orbital Sciences Corporation, Dulles, VA

| | | |
|---|---|---|
| 1400<br>AIAA-2010-3521<br>Theta- D Filter Versus Nonlinear Filtering Techniques in Nonlinear Target Tracking Applications<br><br>Q. Lam and B. Anderson, Orbital Sciences Corporation, Dulles, VA; and M. Xin, Mississippi State University, Mississippi State, MS<br><br>SEE FIRST PAGE » | 1430<br>AIAA-2010-3522<br>Preserving Spacecraft Attitude Control Accuracy Using Theta- D Controller Subject to Reaction Wheel Failures<br><br>Q. Lam and B. Anderson, Orbital Sciences Corporation, Dulles, VA; M. Xin, Mississippi State University, Mississippi State, MS<br><br>SEE FIRST PAGE » | 1500<br>AIAA-2010-3523<br>Investigation of Adapt<br>Reconfiguration Subje<br><br>Q. Lam, Orbital Scien<br>M. Oppenheimer, U. S<br>Laboratory, Wright-Pa<br><br>SEE FIRST PAGE » |

**Session 76- I@A-76** **Space Automation and Robotics I**

Chaired by: W. CHUN, Lockheed Martin Corporation, Highlands Ranch, CO

| | | |
|---|---|---|
| 1400<br>AIAA-2010-3524<br>On- Orbit Assembly of Flexible Space Structures with SWARM | 1430<br>AIAA-2010-3525<br>Avoidance Maneuver Planning Incorporating Station- Keeping Constraints and Automatic Relaxation | 1500<br>AIAA-2010-3526<br>Spacecraft Proximity Operation Em<br>Systems |

| | | |
|---|---|---|
| J. Katz, S. Mohan and D. Miller, Massachusetts Institute of Technology, Cambridge, MA<br>SEE FIRST PAGE | J. Mueller, P. Griesemer and S. Thomas, Princeton Satellite Systems, Plainsboro, NJ<br>SEE FIRST PAGE | M. Majji, J. Davis, J. Doebbler, J. Tu University, College Station, TX; J. F University, Chapel Hill, NC<br>SEE FIRST PAGE |

**Session 77- I@A-77** **Topics in Integrated Systems Health Management I**

Chaired by: R. MAH, NASA Ames Research Center, Moffett Field, CA

| | |
|---|---|
| 1400<br>AIAA-2010-3527<br>The Design of a HSMM- Based Operator State Modeling Display<br><br>R. Castonia, Y. Boussemart, and M. Cummings, Massachusetts Institute of Technology, Cambridge, MA<br>SEE FIRST PAGE | 1430<br>AIAA-2010-3528<br>Damage Mitigation: Recent Advances in Thermopl<br><br>K. Gordon, D. Working, K. Wise, P. Bogert, S. Britt Research Center, Hampton, VA<br>SEE FIRST PAGE |

**1530 - 1600** **Networking Coffee Break**

**Session 78- I@A-78** **Applications Of Guidance, Navigation, & Control II**

Chaired by: D. ACCARDO, University of Naples "Federico II", Naples, Italy, and D. CLANCY, Lockheed Martin Corporation, Fort

| | | |
|---|---|---|
| 1600<br>AIAA-2010-3530<br>Gain Scheduling Based PID Controller for Fault Tolerant Control of Quad-Rotor UAV<br><br>A. Milhim and Y. Zhang, Concordia University, Montréal, Canada; and C. Rabbath, Defense Research and Development Canada, Valcartier, Canada<br>SEE FIRST PAGE | 1630<br>AIAA-2010-3531<br>Improvement of Attitude Estimation Using Hidden Markov Model Classification<br><br>C. Kang and C. Park, Seoul National University, Seoul, South Korea<br>SEE FIRST PAGE | 1700<br>AIAA-20<br>Adaptive for Aircra<br><br>K. Senth Anna Ur |

**Session 79- I@A-79** **Infotech R&D for Unmanned and Robotic Air Systems II**

Chaired by: M. FRANCIS, United Technologies Research Center, East Hartford, CT

| | | |
|---|---|---|
| 1600<br>AIAA-2010-3533<br>Free- Form Command and Control of Robotic Platforms<br><br>P. Scerri, Carnegie Mellon University, Pittsburgh, PA; D. Van Brackle, Lockheed Martin Corporation, Kennesaw, GA; H. Dick and K. Vallandingham, Lockheed Martin Corporation, Leavenworth, KS; and C. Rouff, Lockheed Martin Corporation, Arlington, VA<br>SEE FIRST PAGE | 1630<br>AIAA-2010-3534<br>Development of a Helicopter Deployable Robotic System for Survey and Sampling of Radiological Material<br><br>M. Rose, K. Kochersberger and B. McCabe, Virginia Polytechnic Institute and State University, Blacksburg, VA<br>SEE FIRST PAGE | 1700<br>AIAA-2010-3535<br>Unmanned systems high- level architecture for full interoperability within a network enabled capability<br><br>I. Panella, SELEX Galileo, Basildon, Great Britain<br>SEE FIRST PAGE |

**Session 80- I@A-80** **Intelligent Data Processing II**

Chaired by: R. SAVELY, NASA Johnson Space Center, Houston, TX

| | | |
|---|---|---|
| 1600<br>AIAA-2010-3537 | 1630<br>AIAA-2010-3538 | 1700<br>AIAA-20: |

| | | |
|---|---|---|
| Classifying Acoustic Emission Data in Structural Health Monitoring Using Support Vector Machines<br><br>A. Esterline, K. Krishnamurthy, M. Sundaresan, T. Alam, and D. Rajendra, North Carolina A&T State University, Greensboro, NC<br><br>SEE FIRST PAGE | A Wireless Multiagent Architecture for Structural Health Monitoring that Incorporates Web Services<br><br>A. Esterline, W. Wright, and M. Sundaresan, North Carolina A&T State University, Greensboro, NC<br><br>SEE FIRST PAGE | WITHDR<br>Stochast<br>Survivab<br>Analyses<br><br>J. Castet<br>of Techn |

**Session 81- I@A-81** **Neural Network and Fuzzy Logic Methods II**

Chaired by: K. COHEN, University of Cincinnati, Cincinnati, OH

| | |
|---|---|
| 1600<br>AIAA-2010-3540<br>A Review of Biologically Plausible Neuron Models for Spiking Neural Networks<br><br>L. Long and G. Fang, Pennsylvania State University, University Park, PA<br><br>SEE FIRST PAGE | 1630<br>AIAA-2010-3541<br>Application of Proper Orthogonal Decomposition and Neural<br>Assignment<br><br>K. Cohen, University of Cincinnati, Cincinnati, OH; S. Rasmu<br>Beavercreek, OH<br><br>SEE FIRST PAGE |

**Session 82- I@A-82** **SDRE Approach for Robust Estimation and Control II**

Chaired by: Q. LAM, Orbital Sciences Corporation, Dulles, VA

| | |
|---|---|
| 1600<br>AIAA-2010-3542<br>Dual- Loop Augmented State- Dependent Riccati Equation Control for a Helicopter Model<br><br>A. Bogdanov, Teledyne Scientific & Imaging, Thousand Oaks, CA<br><br>SEE FIRST PAGE | 1630<br>AIAA-2010-3543<br>Indirect Robust Control of Spacecraft via<br>Solution<br><br>M. Xin and H. Pan, Mississippi State Un<br><br>SEE FIRST PAGE |

**Session 83- I@A-83** **Space Automation and Robotics II**

Chaired by: J. LITT, NASA Glenn Research Center, Cleveland, OH

| | | |
|---|---|---|
| 1600<br>AIAA-2010-3544<br>3- D Simulations for Testing and Validating Robotic-Driven Applications for Exploring Lunar Poles<br><br>S. Williams, S. Remy and A. Howard, Georgia Institute of Technology, Atlanta, GA<br><br>SEE FIRST PAGE | 1630<br>AIAA-2010-3545<br>Development of a Mobile Arctic Sensor Node for Earth- Science Data Collection Applications<br><br>S. Williams, M. Hurst and A. Howard, Georgia Institute of Technology, Atlanta, GA<br><br>SEE FIRST PAGE | 1700<br>AIAA-2010-3546<br>Improvements To Sat<br>Measurements Using<br>Techniques<br><br>L. Parker, B. English,<br>Georgia Institute of Te<br><br>SEE FIRST PAGE |

**Session 84- I@A-84** **Topics in Integrated Systems Health Management II**

Chaired by: R. MAH, NASA Ames Research Center, Moffett Field, CA

| | |
|---|---|
| 1600<br>AIAA-2010-3547<br>Fault Detection Isolation & Recovery (FDIR) Lessons Learned<br><br>B. Ferrell and M. Lewis, NASA Kennedy Space Center, Cape Canaveral, FL; R. Oostdyk and J. Goerz, ASRC Aerospace, Cape Canaveral, FL; J. Perotti and B. Brown, NASA Kennedy Space Center, Cape Canaveral, FL | 1630<br>AIAA-2010-3548<br>Functional Fault Modeling of a Cryogenic System fo<br>Isolation<br><br>R. Oostdyk, ASRC Aerospace, Cape Canaveral, FL<br>Space Center, Cape Canaveral, FL; M. Lewis, NAS |

| | |
|---|---|
| SEE FIRST PAGE » | Cape Canaveral, FL; and J. Perotti, NASA Kennedy FL<br><br>SEE FIRST PAGE » |